



## REVIEW



Cite this: *J. Mater. Chem. A*, 2017, 5, 17777

## Graphene as a flexible electrode: review of fabrication approaches

Russell Kai Liang Tan,<sup>†a</sup> Sean P. Reeves,<sup>†a</sup> Niloofar Hashemi,<sup>b</sup> Deepak George Thomas,<sup>a</sup> Emrah Kavak,<sup>a</sup> Reza Montazami <sup>\*a</sup> and Nicole N. Hashemi <sup>†\*a</sup>

In recent years, the technological advancement of supercapacitors has been increasing exponentially due to the high demand in electronic consumer products. As so, researchers have found a way to meet that demand by fabricating graphene. As developments are made toward the future, two big advancements to be made are large-scale fabrication of graphene and fabricating graphene as a flexible electrode. This would allow for use in larger products and for manipulation of the unique properties of graphene to accommodate superior design alternatives. While large scale production is still mentioned, this review is specifically focusing on different methods used to fabricate graphene as a flexible electrode. Various fabrication methods, such as Hummers' method, chemical vapor deposition, epitaxial growth, and exfoliation of graphite oxide, used to fabricate graphene in such a way that allows flexibility and utilization of graphene's mechanical and electrical properties are discussed. Additionally, a section on environmentally friendly fabrication approaches is presented and discussed.

Received 3rd July 2017  
Accepted 28th July 2017

DOI: 10.1039/c7ta05759h

rsc.li/materials-a

## 1 Introduction

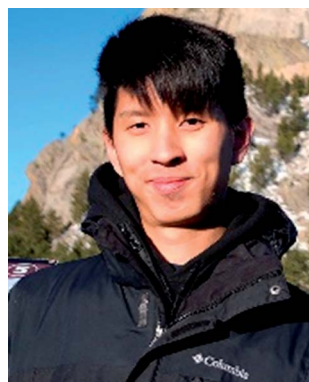
Since the discovery of graphene and its electrical and mechanical potential over ten years ago, it has been studied and manipulated in the attempt to further technology for the future. Graphene, which are carbon atoms bonded in a honeycomb lattice structure in sheet form with the thickness of one atom,

has many factors that go into fabrication, as well as serving as a multi-functional material. It has the capabilities to assist in transistors, electrodes, sensors, and many more applications. The purpose of this study is to focus on graphene used as an electrode with flexible characteristics. The goal alongside that purpose is for researchers to use this as a resource to assist in their fabrication of graphene, while moving away from past ways that restrict an electrode potential to be more flexible, more powerful, and significantly smaller. Indium tin oxide (ITO) has been commonly used in applications of transparent electrodes. ITO does not have characteristics to be used as a flexible transparent electrode. This is because of its film brittleness and low infrared transmittance. These

<sup>a</sup>Department of Mechanical Engineering, Iowa State University, Ames, IA 50011, USA.  
E-mail: reza@iastate.edu; nastaran@iastate.edu

<sup>b</sup>Department of Materials Science and Engineering, Sharif University of Technology, Tehran, Iran

<sup>†</sup> R. K. T and S. P. R. contributed equally.



*Russell Tan is a Mechanical Engineering student at Iowa State University. His research skills involve fluids, immeso-geometric analysis, and control systems.*



*Sean Reeves is a Mechanical Engineering student at Iowa State University. His research is focused on chemistry and hydraulics.*

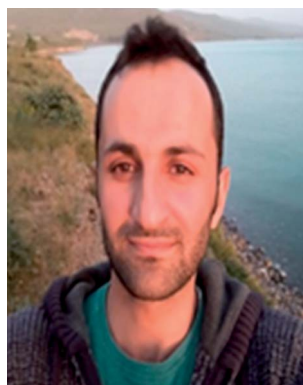
characteristics, along with the scarcity of indium and high overall cost prevents the development of future applications.<sup>1</sup> Because of graphene's incredible mechanical and electrical properties, as well as its size, it has great potential to further application development. One of graphene's outstanding properties is the thermal conductivity ( $\kappa$ ) due to the high levels of phonon-dominated on the surface, which can be increased with the switch-on phenomenon and subtracting the defect levels in graphene.<sup>2,3</sup> With research and development reaching a global scale, this review contains compilation and analysis of different fabrication methods and techniques used to fabricate graphene as a flexible electrode. The following information does not describe the only ways to fabricate graphene as an electrode, but they are the most common methods to take to obtain successful results. In taking the steps toward moving away from past methods and furthering graphene for industrial application, there are a few challenges that are faced. Some of these challenges include large-scale production inability, production costs, and producing it with flexible characteristics. Most synthesis practices continue for a long time and result in high cost and poor scalability in real-world applications.<sup>4</sup> For example, for optoelectronic and electrochemical devices, inorganic semiconductors are considered for research and

exploration of micro- and nanoscale phenomena and learning the importance of size and dimensionality.<sup>5</sup> Due to their low work functions, high aspect ratios, and high mechanical stability, the essential nanostructure design of various inorganic semiconductors offers exceptional features for a wide range of systems used in electronic applications. There have been many advances in application of graphene in physics, whereas its application in chemistry, biochemistry and bio-sensing needs development. The positive environmental impact that graphene can have is significant too. For example, with a constant increase in freshwater resource contamination, graphene can assist in the desalination of seawater into purified water through capacitive deionization and the graphene mixture used as the positive electrode.<sup>6</sup>

Graphene usage for sensors has been reported numerous times in applications such as strain-sensors or efficient human-motion detection, whereas for electrodes, graphene's usage has mainly been reported on the detection of small biologically relevant analytes. Batteries are also a great example of applications that graphene can benefit. Graphene proves to be an excellent alternative to the commonly used lithium ion battery. With the inspiration of metal-air batteries, which relies on its open structure to generate electricity using oxygen gas, *in situ*



*Niloofar Hashemi is an Adjunct Faculty at the Iran University of Applied Science and Technology. She did her undergraduate studies in Materials Science and Engineering at the Sharif University of Technology.*



*Emrah Kavak is a graduate student in the Institute of Science at Van Yuzuncu Yil University. He received his B.S. in Chemistry from Van Yuzuncu Yil University in 2014. His research focuses on synthesis of heterocyclic organic compounds, and design and fabrication of nanomaterials. He is currently a visiting scientist at Iowa State University.*



*Deepak-George Thomas is a graduate student in the Department of Mechanical Engineering at Iowa State University. He completed his Bachelors in Technology from Sir Padampat Singhania University. His research focuses on graphene fabrication and polymer microfibers.*



*Reza Montazami is an Assistant Professor in the Department of Mechanical Engineering at Iowa State University. He received his B.S. in Physics, and M.S. and Ph.D. degrees in Materials Science and Engineering from Virginia Tech, in 2007, 2009, and 2011 respectively. He joined Iowa State University in 2011, and became an Associate Scientist at Department of Energy's Ames Laboratory in 2012. His current research interests include study of functional materials, soft (flexible and stretchable) electronics, mechanics of soft materials, and advanced additive manufacturing of functional polymers and soft electronics.*

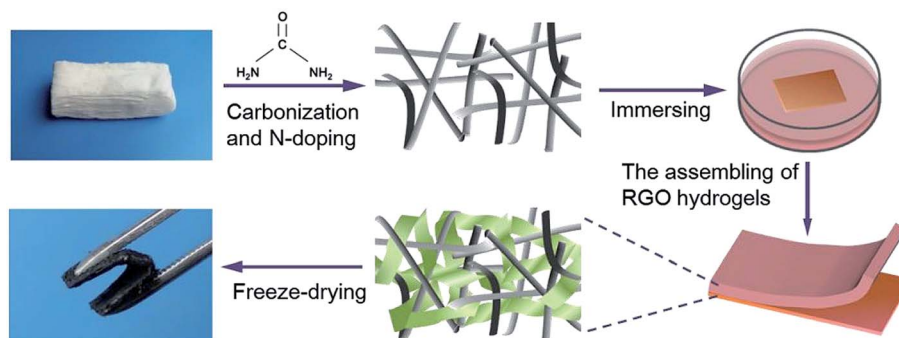


Fig. 1 Preparation of 3D NCCF-rGO electrodes via a facile synchronous reduction and assembly process.<sup>23</sup>

graphene-like carbon nanosheets adopted a similar strategy.<sup>7</sup> It has great potential in point-of-care medical diagnostics, skin-substrate electronics, HMI's, and many more applications.<sup>8</sup> More possibilities include computational framework with tetrahertz operating speeds for compact all-carbon spin logic circuits and drastically improved in power delay products.<sup>9</sup> It also makes for improved use in electronic devices like touch panels, p-n junction materials, wearable technology and hydrogen storage materials.<sup>1,10–12</sup> The possibilities are endless once the fabrication of graphene as electrodes becomes more controllable (Fig. 1).

## 2 Fabrication methods

There are plenty of ways that graphene can be fabricated, especially as research on graphene's multi-use capabilities reach various applications at an exponential rate. For the case of graphene fabrication as a flexible electrode, there are four methods that are commonly used today. These methods are a modified Hummers' method, exfoliation of graphite oxide, chemical vapor deposition, and epitaxial growth. Each fabrication method can be approached from different angles. These approaches may include, but are not limited to, hybrid solutions, using different elements, or manipulating material mass or volume. Other methods to note are facile photochemical strategies for rapid construction of porous graphene frameworks and template methods using a triblock copolymer as a template for fabrication (Table 1).<sup>13</sup>



*Nicole Nastaran Hashemi is an Assistant Professor in the Department of Mechanical Engineering at Iowa State University. Her research interests are in the areas of microfluidics, nanostructures, and biomaterials. She has received her Ph.D. in Mechanical Engineering from Virginia Tech in 2008.*

### 2.1 Modified Hummers' method

Hummers' method is a very common method in the process of fabricating graphene. Graphite oxide is created mainly by the chemical oxidation of graphite. It is originally synthesized by an addition of potassium chlorate to a graphite/HNO<sub>3</sub>/H<sub>2</sub>NO<sub>3</sub> mix.<sup>14</sup> These are known as the Staudenmaier and Brodie methods. Hummers' method was later developed, in which KMnO<sub>4</sub> and NaNO<sub>3</sub> were dissolved in concentrated H<sub>2</sub>SO<sub>4</sub> to allow for a more effective oxidation for graphite to produce graphite oxide. The cons of both the Staudenmaier and Brodie methods were the long turnover rate of 4 days, and the consumption of toxic and harmful gases.<sup>15,16</sup> The difference between the two methods is that Hummers' method takes only a few hours (Fig. 2).

Modifications have been made to Hummers' method to address problems that have risen, like adding a peroxidation step, or removing NaNO<sub>3</sub> from the method and finding a replacement due to its toxic gas generation. Each version of Hummers' method was modified in different ways and it depends on the user as to what modifications can be made. To fabricate graphene, Hummers' method is usually used since the graphite must be oxidized (unless a unique direction is taken like the R2R approach explained later).

One example of a general Hummers' method consists of graphite powder stirred and chilled with H<sub>2</sub>SO<sub>4</sub> and NaNO<sub>3</sub>.<sup>17</sup> During stirring, KMnO<sub>4</sub> was added in aliquots over 2 hours, followed by room temperature cooling after the stirring process was completed. Then, 35 °C was applied for 30 minutes, followed by adding the solution into a flask with deionized water. The temperature was again increased to 70 °C, and the time to 15 min. The new solution was added to a larger volume of deionized water, where H<sub>2</sub>O<sub>2</sub> was added to remove the KMnO<sub>4</sub>. Deionized water repetition was necessary until a neutral pH was achieved. GO was then present and was dried in a vacuum for 2 days at 60 °C (Fig. 3).

Like previously mentioned, each Hummers' method could be modified in certain ways. An example of a modified Hummers' method is as follows.

Firstly, a PANI/GN composite was acquired. To do that, an aqueous GN dispersion (1.0 mg mL<sup>-2</sup>) was prepared using a modified Hummers' method. A solution of 0.4 mL aniline monomer (solvent: 2 M HCl, 25 mL) was dropped into the as-

**Table 1** A summary of graphene fabrication property outcomes. ✓ denotes that the fabrication method provides this property. ✗ denotes that the fabrication method does not provide this property

	Electrical conductivity	Strength	Elasticity	Large surface areas	Chemically inert	Transparency	Short fabrication time	Large output volume
Hummers' method	✓	✓	✗	✗	✓	✓	✓	✓
Exfoliation of graphite oxide	✓	✓	✗	✗	✓	✗	✓	✗
CVD	✓	✓	✓	✓	✓	✓	✗	✓
Epitaxial growth	✓	✓	✓	✓	✓	✓	✓	✓

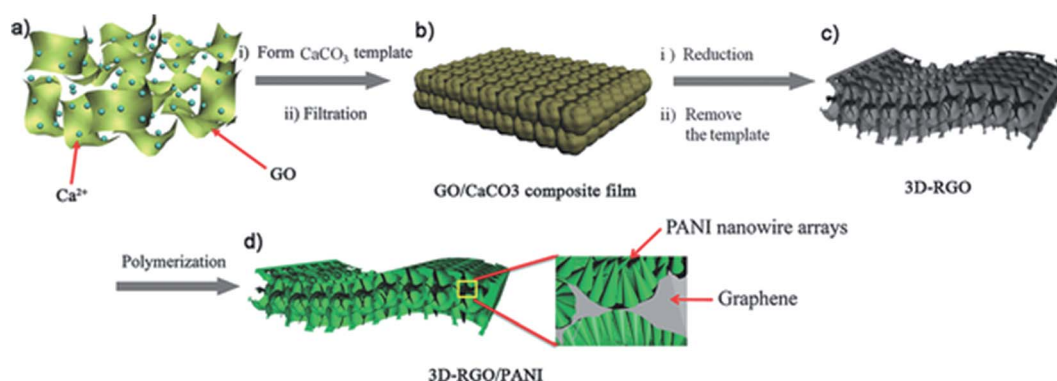


**Fig. 2** Preparation of the 3D-rGO and 3D-rGO/PANI films. (a) Mixture of  $\text{CaCl}_2$  with GO dispersion. (b) Undergo precipitation and vacuum filtration to get GO/ $\text{CaCO}_3$  composite films. (c) Reduction and removal of  $\text{CaCO}_3$  to form a 3D graphene structure. (d) Polymerization of a 3D graphene structure to obtain hierarchical PANI/graphene composites.<sup>39</sup>

prepared GN suspension (25 mL); afterwards the mixture was sonicated for 0.5 hours, mixed with  $\text{HCOOH}$  and then strongly mechanically stirred for 0.5 hours. Subsequently, 50 mL of 240 mg ammonium persulfate (solvent: 1 M  $\text{HCl}$ ) was added dropwise into the above mixture and stirred in an ice-water bath for 2 hours to form a PANI/GN suspension. The next step was to synthesize PANI/GN to BC to form a film like electrode. Firstly, the gel-like white BC pellicles were washed thoroughly with deionized (DI) water, then cut into small slices, and subsequently pulped with a mechanical homogenizer at the speed of 10 000 rpm to obtain the BC suspension ( $0.7 \text{ mg mL}^{-1}$ ). The resultant BC suspension (200 mL) was drained on a nitro cellulose filter membrane (porous size of  $0.22 \mu\text{m}$ ) to get a uniform BC paper by vacuum filtration. Next, the obtained PANI/GN dispersion was decanted onto the prepared BC paper to form a flexible film, and the fabricated film was washed several times with DI water. After the wet film was dried at  $55^\circ\text{C}$  for 8 hours and then peeled off to get the freestanding PANI/GN/BC paper. Three different abbreviations, namely PANI(L/M/H)/GN/BC represented the various concentrations of PANI for 0.2, 0.3 and 0.4 mL. An *in situ* polymerization and vacuum filtration strategy was employed to coat a uniform layer of PANI onto the GN surface, followed by pouring onto BC paper to form the flexible and freestanding film. Because of the abundant groups of BC and its excellent physical properties, PANI/GN composites could strongly bind with the BC paper *via* hydrogen bonding and electrostatic interaction. The mixture was fully immersed and utilized the porous network of BC to obtain large mass loadings.<sup>18,19</sup>

A high demand for on-body wearable medical apparatus and implantable devices also used Hummers' method in its experiment.<sup>20</sup> The research described a flexible graphene electrode based on graphene paper (GP) supported 3D monolithic nanoporous gold (NPG) scaffold (NPG/GP), with modifications made to provide a high density, well dispersed, ultrafine binary PtCo alloy nanoparticles through ultrasonic deposition. The first step was to fabricate a freestanding graphene oxide (GO) *via* a modified Hummers' method, which was included in the author's recent work.<sup>21</sup> Freestanding GO paper was fabricated starting by dropping a well dispersed GO solution ( $5 \text{ mg mL}^{-1}$ ) onto a commercial printing paper surface (A4). The GO solution was then spread uniformly across the commercial printing paper *via* rolling multiple times. The sample was allowed to air dry to obtain a uniform GO paper. A reduction process for GO paper was carried out by soaking it in HI solution (45 wt%) for 10 minutes at room temperature. During this process, bubbles emitted from the cellulose papers allowed the thin film to peel by itself. Then, the rGO paper was rinsed with a saturated sodium bicarbonate solution, water and methanol followed by vacuum drying at  $80^\circ\text{C}$ . The rGO paper was then coated with a layer of PANI *via in situ* polymerization. Generally, the PANI nanofiber network was synthesized with a two-step method on a three-electrode system in a 1 M  $\text{HCl}$  electrolyte and 0.3 M aniline monomer. Nucleation of PANI was performed with a constant feed of a voltage at 0.8 V for 1 minute at room temperature. The following step allowed nanowires to grow under a constant current condition with current density of  $2 \text{ mA cm}^{-2}$ . The resultant PANI layer was then covered with an

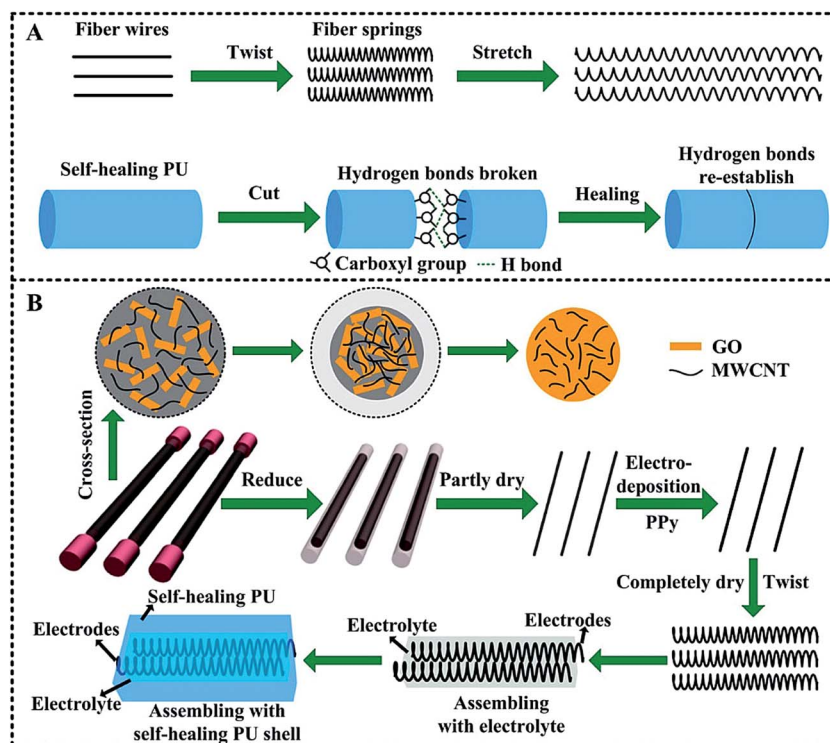


Fig. 3 Schematic diagram of the highly stretchable and healable fabrication process. (A) The twisting process of rGO fibers into springs. (B) Preparation procedures of the rGO/MWCNT PPy-decorated supercapacitors.<sup>48</sup>

ultrathin GO film through a dip-coating method. The last step was to take the aforementioned sample and soak it in HI solution for a few minutes at room temperature to produce rGO/PANI/rGO paper. The next step was to fabricate freestanding NPG/GP by immersing a piece of Ag–Au leaf (1 cm × 1 cm) into concentrated nitric acid to float the leaf at the air–liquid interface. After the leaf was observed to float freely on the solution surface, the glass slide was removed. Then, the leaf was dealloyed for 6 hours in the dark at 30 °C. Subsequently, the leaf was removed from the acidic solution using a glass slide and rinsed with deionized water by allowing it to float three times (15 minutes for one time). The NPG film was then transferred to a freestanding GP, and 10 µL Nafion solution was dropped

on the surface of the NPG to obtain a freestanding GP supported NPG (NPG/GP). To get a freestanding PtCo/NPG/GP, the NPG/GP was allowed to undergo PtCo alloy nanoparticles electrochemical deposition under ultrasonic irradiation (45 W).<sup>22</sup> The aforementioned process was performed in 0.2 M of Na<sub>2</sub>SO<sub>4</sub> containing 5 mM H<sub>2</sub>PtCl<sub>6</sub> · 6H<sub>2</sub>O and 15 mM CoCl<sub>2</sub> · 6H<sub>2</sub>O using a cyclic voltammetry technique at a range of –1.0 to 0.0 V and a scan rate of 250 mV s<sup>-1</sup>. The resultant nanohybrid paper electrodes were then cleaned carefully with distilled water and dried at room temperature (Fig. 4).

Aerogels and graphene were both interesting materials that were highly sought after for research purposes. One experiment incorporated graphene aerogels into a low-cost 3D N-doped

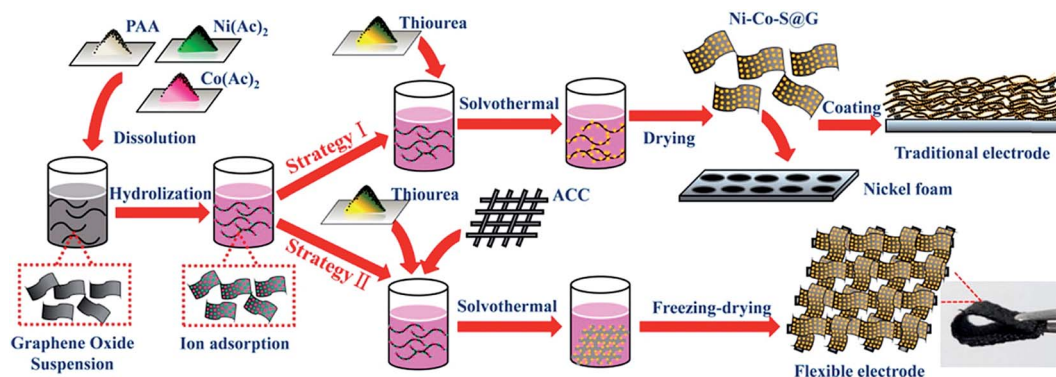


Fig. 4 Schematic fabrication process detailing one-step solvothermal method to obtain Ni–Co–S@G and Ni–Co–S@G/ACC electrodes as (Strategy I) and (Strategy II), respectively.<sup>70</sup>

biomass-derived carbon framework as a potential flexible energy storage.<sup>23</sup> The 3D structural framework potentially boosts the energy storage device with superb electrical conductivity, chemical stability and flexibility.<sup>24,25</sup> Firstly, GO was fabricated using a modified Hummers' method. 2 g of graphite was added into 120 mL of sulfuric acid (98%) in an ice bath and cooled to 0 °C under stirring. Then, 1 g of NaNO<sub>3</sub> (AR) was added and stirred for 30 minutes. Subsequently, 6 g of KMnO<sub>4</sub> (AR) was slowly added to the solution and stirred for 2 hours to maintain the temperature below 20 °C. Next, 150 mL of deionized water was added, followed by 200 mL of H<sub>2</sub>O<sub>2</sub> (38%) dropwise. The resulting mixture was then washed with deionized water and HCl (5%) to obtain an aqueous GO dispersion. The next step was to synthesize N-doping cotton-derived carbon frameworks (NCCF). In this step, raw cotton was used without any pre-treatment. Urea was mixed with a piece of cotton (mass ratio of 4 : 1) in a quartz boat, followed by carbonizing at 800 °C for 1 hour at the rate of 5 °C min<sup>-1</sup> in a N<sub>2</sub> atmosphere. The high temperature N<sub>2</sub> atmosphere allowed the decomposition of urea to react with the carbonized NCCF. The resulting product was further treated with ultrasonication for 1 hour in the presence of HNO<sub>3</sub>/H<sub>2</sub>SO<sub>4</sub> (v/v = 1/3). The finalized sample was then cleaned with deionized water and dried at 90 °C overnight. The final step was to synthesize NCCF-rGO. A piece of NCCF was cut from the acid treated cotton according to its natural texture. Next, Cu foil and a NCCF piece was immersed into acidified GO solution (3 mg mL<sup>-1</sup>, 0.001 M HCl) to obtain the gel of NCCF. The thin piece of NCCF was to be strongly bound to the Cu foil for 6 hours, allowing interfacial gelation of GO to be self-assembled into hydrogels of the Cu foils. After that, the resulting sample was carefully cleaned with deionized water to remove the unreacted GO solution. After the aforementioned step, the sample was immersed into 10 fold diluted HCl solution to detach the gel of the NCCF from Cu foil followed by washing it with 20 fold diluted aqueous HCl and deionized water respectively to remove any remaining chemical residues. Subsequently, the sample was freeze-dried to obtain an aerogel-like dried product, followed by annealing it at 300 °C for 1 hour under a N<sub>2</sub> atmosphere (Fig. 5).

The usage of polypyrrole (PPy) was shown by how researchers experimented on fabricating hybrid paper electrode with rGO (using NaBH<sub>4</sub>), *in situ* polymerization of PPy and cellulose.<sup>26</sup> The experimenters used *in situ* polymerization of PPy and chemical reduction with NaBH<sub>4</sub> to reduce graphene oxide. Paper proved to be an ideal base for flexible supercapacitor fabrication, since paper could easily synergize with a wide range of

electrochemically active substances such as electronically conducting polymers (ECPs).<sup>27-31</sup> Polypyrrole (PPy), polyaniline (PANI) and poly(3,4-ethylenedioxythiophene) (PEDOT) are examples of ECPs that possessed high pseudocapacitance, quicker redox switching, light weight, high conductivity and low costs, crowning these materials as high tier class materials for high-performance supercapacitors.<sup>32-37</sup> The first part of fabricating PPy/cellulose paper required the base cellulose paper with dimensions roughly 40 mm × 40 mm to be soaked in four different concentrations of a pyrrole monomer at 0.05, 0.15, 0.45 and 1.35 M for 2 hours. Subsequently, an aqueous solution of iron(III) chloride hexahydrate (FeCl<sub>3</sub> · 6H<sub>2</sub>O) was added slowly into each individual concentrations of the pyrrole monomer to act as an oxidant for *in situ* polymerization process for 3 hours. The molar ratios of the ferric iron/pyrrole are 0.1, 0.3, 1 and 3 respectively. The resulting 16 PPy/cellulose papers were placed into 1 M HCl for 30 minutes and then rinsed with distilled water, followed by drying in a vacuum oven at 50 °C for 24 hours. The next step was to fabricate GO through a modified Hummers' method. 2 g of graphite powder was mixed into 80 mL of sulphuric acid and 4 g of sodium nitrate, under magnetic stirring in an ice bath. 8 g of potassium permanganate was added to the resulting suspension under intense agitation. The temperature of the mixture was then brought down to 0 °C for 3 hours, followed by stirring at 40 °C for 2 hours. Then, 200 mL of deionized water was added into the resultant mixture, followed by its heating to 98 °C for 30 minutes. Then, 30 mL of H<sub>2</sub>O<sub>2</sub> (30%) was added into the solution, followed by rinsing it with 200 mL of 5 wt% HCl at deionized water. The final product would be graphite oxide, which would be immediately subjected to a facile ultrasonication treatment that exfoliated the graphite oxide to GO. To fabricate rGO/PPy/cellulose (RPC) papers, PPy/cellulose papers with the lowest sheet resistance were picked and separated in three different concentrations of GO dispersions (0.1, 0.5 and 2.5 g L<sup>-1</sup>). GO dispersions was prepared under ultrasonication for one hour (500 W) in an ice bath. The resulting GO/PPy/cellulose papers was reduced with 0.15 M of aqueous NaBH<sub>4</sub> solution, then stirred for 12 hours. The resulting RPC papers were then cleaned with deionized water to remove any impurities on the surface, followed by drying at 50 °C for 24 hours. The assembly of the all-solid-state flexible laminated symmetric supercapacitor (SSC) is fairly simple, involving just pressing two RPC papers dipped in a H<sub>3</sub>PO<sub>4</sub>/PVA gel electrolyte together followed by transferring it to a fume hood at room temperature to allow excess water to evaporate. The aforementioned gel electrolyte was prepared by adding 6 g

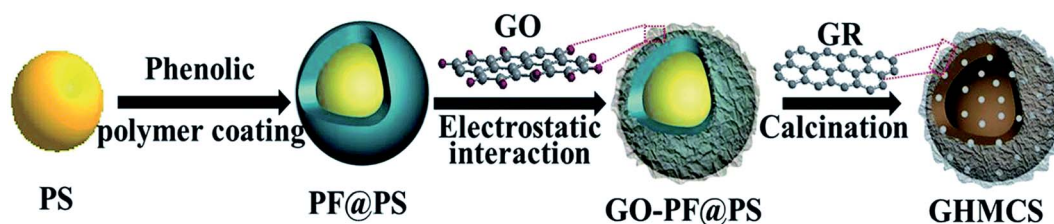


Fig. 5 An illustration of the fabrication process of graphene coated hollow mesoporous carbon spheres (GHMCSs).<sup>83</sup>

of  $\text{H}_3\text{PO}_4$  and 6 g of PVA in 60 mL of deionized water under magnetic stirring at  $85^\circ\text{C}$  until the solution becomes transparent (Fig. 6).

In an experiment that investigated a graphene/polyaniline@carbon cloth composite as a supercapacitor *via* a simple one-step electrochemical co-deposition process, it was realized that graphene oxide to graphene/polyaniline composite must be prepared to make the supercapacitor achievable.<sup>38</sup> The synthesis of GO through the oxidation of graphite flakes was done *via* a modified Hummers' method. The resulting GO dispersion was placed in a centrifuge at 4000 rpm for 30 minutes to remove remaining aggregates followed by dialysis to purify salt impurities for 1 week. The GO dispersion was then adjusted to  $0.36\text{ mg mL}^{-1}$  for later experiments. To remove any grease and impurities, a carbon cloth (1 cm  $\times$  2 cm) was soaked in acetone and distilled water followed by sonication for 30 minutes. The aforementioned process was repeated several times followed by a drying process in vacuum at  $60^\circ\text{C}$ . Then, a transparent solution was prepared by adding 135 microl of aniline into 10 mL of distilled water and sonicating it until it became transparent in room temperature. The electrolyte for electrochemical co-

deposition was created by adding 1 mL of 1.0 M  $\text{Na}_2\text{SO}_4$  and the previous sonicated solution into 15 mL of GO dispersion, to be further sonicated again for 10 minutes. A three-electrode system was conducted using carbon cloth, Pt foil and Ag/AgCl as the working electrode, counter electrode and reference electrode respectively. Three different samples needed a slight modification in settings for cyclic voltammetry (CV) cycles, namely GP@cc (the sample before this), PANI@cc and rGO@cc with voltage ranges at  $-1.2$  to  $0.8\text{ V}$ ,  $0$  to  $0.8\text{ V}$  and  $-1.2$  to  $0\text{ V}$ , respectively. All samples used a scan rate of  $2\text{ mV s}^{-1}$ . After each cycle, the samples were cleaned with distilled water and repeated multiple times to remove the absorbed monomer or salts (Fig. 7).

One team<sup>39</sup> experimented on fusing graphene and a polyaniline (PANI) composite film together to further study graphene and nanostructured pseudocapacitance materials.<sup>40,41</sup> Graphene is known to have a stable but low capacitance due to graphene adopting the electric double-layer capacitor mechanism that aids in energy storage.<sup>42-44</sup> PANI is well known to be a good candidate for supercapacitor with pseudocapacitance materials because of characteristics such as environmental stability, doping/dedoping chemistry and a special conducting mechanism.<sup>45-47</sup> Preparation of materials for this experiment is simple; all other reagents mentioned would be of AR grade and aniline was distilled before use. GO was obtained *via* a modified Hummers' method. The first step was to fabricate freestanding 3D-rGO film. GO solid was dispersed with ultrasonication for 100 minutes and centrifuged at 400 rpm to obtain approximately  $1.25\text{ mg mL}^{-1}$  of GO dispersion. Subsequently, 0.4 mol of  $\text{CaCl}_2$  and 2.5 mL  $\text{NH}_3 \cdot \text{H}_2\text{O}$  was added to the GO dispersion respectively after  $\text{CaCl}_2$  was dissolved completely. The mixture was stirred for 10 minutes and then placed in a  $\text{CO}_2$  atmosphere at a rate of  $1\text{ L min}^{-1}$ . The mixture was allowed to react for 80 minutes, then left to rest overnight. Then, one third of the resultant suspension was allowed to undergo vacuum filtration to obtain a GO- $\text{CaCO}_3$  film. The resultant film was then reduced in hydrazine vapor at  $40^\circ\text{C}$  for 12 hours, cleaned with diluted hydrochloric acid to remove  $\text{CaCO}_3$  particles on the surface and finally washed with deionized water and ethanol to get

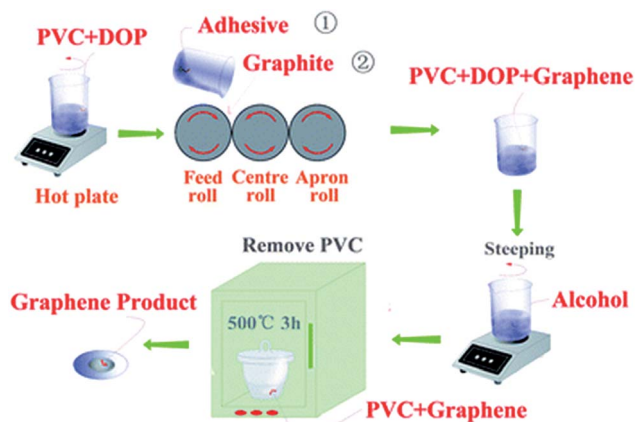


Fig. 6 Depiction of the exfoliation of natural graphite with the three-roll mill system.<sup>84</sup>

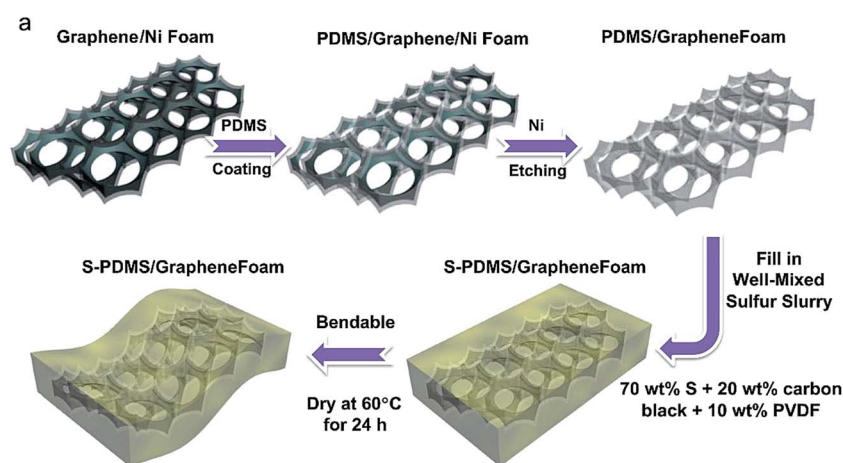


Fig. 7 Schematic of the synthesis procedure to fabricate PDMS/GF and S-PDMS/GF electrodes.<sup>90</sup>

freestanding graphene film. The process to prepare a 3D-rGO/PANI composite film allows 3D-rGO/PANI nanocomposites to be synthesized with 3D-rGO film *via* dilute polymerization. First, 20 mL of 1 mol L<sup>-1</sup> aqueous HClO<sub>4</sub> solution was prepared and poured into a reaction vessel within an ice bath. 5 mL of ethanol was added to the 3D-rGO film and placed next to the reaction vessel to improve the wettability of the film. After the solution cooled down, an aniline monomer was added and stirred for 10 minutes to obtain a homogeneous mixture. (NH<sub>4</sub>)<sub>2</sub>S<sub>2</sub>O<sub>8</sub> (APS) was prepared in 15 mL aqueous HClO<sub>4</sub> solution and precooled (ratio of aniline/APS = 1.5) to act as the oxidant. The oxidant was then added into the monomer solution. The polymerization process started and was sustained for 24 hours in an ice bath. A composite film was obtained by cleaning the sample with deionized water and ethanol, then drying it in room temperature.

Another research team studied reduced graphene oxide based off fiber springs to enhance the flexibility and regenerative capabilities of a supercapacitor.<sup>48</sup> Stretchable electronic devices recently have been a strong interest in the modern electronics market.<sup>49–55</sup> Fiber was incorporated into the supercapacitor as it plays an important role to help boost structural strength that makes it flexible, lightweight and soft at a low cost.<sup>56–58</sup> The combination of fiber and graphene creates graphene fibers, which showcases both high thermal and electric conductivity, superb stiffness and elasticity, and strong stability.<sup>59–62</sup> In practical applications, the graphene fibers would undergo high-stressed environments that pushes the reliability and stability of the supercapacitor. Therefore, the graphene fibers could potentially suffer from mechanical damage, and eventually break down.<sup>63,64</sup> Self-healing was applied to the graphene fiber supercapacitor to heal damaged fibers, allowing it to regain mechanical and structural properties.<sup>65</sup> Not only can those materials heal and restore electrical and structural characteristics of mechanically damaged supercapacitors, it can also prevent structural fractures from happening.<sup>66–68</sup> GO was prepared with oxidized graphite powder using a modified Hummers' method. Multi-walled carbon nanotubes (MWCNTs) and sodium dodecyl sulfate (SDS) was added into 5 mg mL<sup>-1</sup> of aqueous GO solution with a ratio of GO/MWCNTs of 2 : 1, 1 : 1 and 1 : 1.5. The mixture was ultrasonicated to allow even dispersion, followed by addition of vitamin C particles and ultrasonicated once more for 5 minutes. The resulting mixture was injected into 1.5 mm diameter pipes and sealed at both ends with polydimethylsiloxane (PDMS). GO was reduced after heating in an oven at 90 °C for 6 hours and the remaining wet fibers were dried. Partially dried rGO/MWCNT fibers were the base for electrodeposition of PPy according to literature in 1, 1.5 and 2 min.<sup>69</sup> Polypyrrole (PPy) was deposited on rGO/MWCNT fibers using 5% (v/v) pyrrole monomer, 0.2 M NaClO<sub>4</sub> with a constant voltage of 0.8 V. PPy/rGO/MWCNT fibers were physically modified into a spring shaped structure, then followed by coating with a PVA–H<sub>3</sub>PO<sub>4</sub> gel electrolyte and dried under vacuum at room temperature. Then, the springs were placed parallel and coated with the same electrolyte before and dried

under vacuum. The supercapacitor was finally coated with polyurethane (PU) and dried in air.

Using other elements to promote supercapacitor performance is a good approach.<sup>70</sup> This group discussed utilizing nickel cobalt sulfide to promote supercapacitor performance by uniformly dispersing the ncs on the surface of graphene *via* a one-step solvothermal method with poly(acrylic acid) (PAA) additive. Nickel–cobalt sulfides are binary metal sulfides from the transition-metal sulphides (TMSs) group that was recently considered for their rich redox reactions compared to both single component sulfides (NiS<sub>x</sub> or CoS<sub>x</sub>).<sup>71</sup> The downsides of nickel–cobalt-sulfide reported were insufficient capacitance under high rates because of the disadvantageous ion transportation length and low electronic conductivity,<sup>72,73</sup> and poor electrochemical stability from long-term cyclic that creates mechanical stress and strain that eventually causes a large change in volume and structural failure.<sup>74,75</sup> The combination of nickel–cobalt sulfide nanoparticles on graphene (Ni–Co–S@G) delivers outstanding energy densities without sacrificing capacitance or electrochemical stability, since a simultaneous utilization of the active material and contented conductivity can be achieved.<sup>76–78</sup> All chemicals used in this experiment were of AR grade. GO was synthesized with a modified Hummers' method to obtain a GO suspension. The one-step solvothermal synthesis method was used to fabricate Ni–Co–S@G nanocomposite. Ni(CH<sub>3</sub>COO)<sub>2</sub>·4H<sub>2</sub>O, Co(CH<sub>3</sub>COO)<sub>2</sub>·4H<sub>2</sub>O and PAA (*M<sub>w</sub>* = ~2000, Macklin) with a molar ratio of 1 : 2 : 2 : 8 was dissolved in 35 mL 0.5 mg mL<sup>-1</sup> GO suspension in ethylene glycol (EG) at 80 °C under vigorous stirring for 2 hours. Then, thiourea was added to the solution to undergo hydrolysis. The resulting solution was transferred into a 50 mL Teflon-lined stainless steel autoclave at 200 °C for 10 hours. The solution was placed in a centrifuge at 5000 rpm to remove the undecorated particles. The remaining samples were cleaned with deionized water and ethanol multiple times. The Ni–Co–S@G/ACC electrode was fabricated the same way as Ni–Co–S@G except for adding a piece of ACC into the Teflon-lined stainless steel autoclave before the solvothermal process.

One incredibly influential role graphene plays is its ability to act as an electrode in capacitive deionization experiments. Hummers' method can assist in the fabrication of this electrode. One example described GO prepared by Hummers' method and the powder then being ultrasonicated into 3 mg mL<sup>-1</sup> DI.<sup>79</sup> To prepare what was termed GO@PS microspheres using polystyrene, 100 mL of the mix was placed into a prepared aqueous suspension of 50 mL PS microspheres under magnetic stirring. Ultrasonication was carried out for 2–3 hours after. Next, vacuum filtration with a millipore filter was conducted with the resulting mix. The spheres and sheets were peeled from the filter and dried at 40 °C. The resulting composites were annealed at 550 degrees C for an hour. Next, under N<sub>2</sub>, the same was done at 900 degrees C and a heating rate of 1 degree C min<sup>-1</sup>. This reduces the GO into graphene and the PS spheres are taken away. The final resultant material is termed 3DMGA. As expected, there are many other ways to fabricate graphene as an electrode for the improvement of capacitive deionization,



including sulfonic and amine function groups on 3D graphene, as well as dual-template prepared carbon composites.<sup>80,81</sup>

An example discussed on the usage of graphene-coated hollow mesoporous carbon spheres (GHMCSs) as electrodes for capacitive deionization (CDI). A template-directed method was used to fabricate GHMCSs, where a phenolic polymer coated polystyrene spheres were used as the template. As a result, the graphene composite formed a hierarchically porous nanostructure, with individual hollow mesoporous carbon spheres uniformly distributed across graphene sheets. To fabricate GHMCSs, phenolic polymer coated polystyrene spheres (PF@PS) were synthesized. PS sphere procedures were previously reported with a diameter of 180 nm.<sup>82</sup> 150 mg of PS spheres were dispersed into 50 mL of deionized water, followed by 20 mL of aqueous phenol solution (0.188 g) and 10 mL of hexa-methylenetetramine (0.14 g). The solution was gently stirred for 15 minutes and transferred into a 100 mL Teflon-lined autoclave at 160 °C for 4 hours. PS@PF spheres was obtained after centrifugation and cleaned with deionized water and pure ethanol. The next procedure was to synthesize GO with PF@PS nanospheres. GO was prepared *via* Hummers' method. A 3 wt% aqueous suspension of the PF@PS nanospheres were obtained by re-dispersing them into deionized water. 20 mL of GO dispersion was added into 6 g of aqueous suspension of PF@PS under magnetic stirring conditions. The solution was ultrasonicated for 1–2 hours to obtain a homogeneous colloidal suspension of PF@PS and GO hydrosol. The assembly of PF@PS nanospheres and GO sheets was achieved by vacuum filtration using a millipore filter. The resulting GO–PF@PS composite from vacuum filtration was peeled off from the filter and air-dried overnight at 40 °C. Then, the composite was annealed in a tubular furnace at 150 °C for 1 hour, followed by 900 °C for 2 hours under a N<sub>2</sub> atmosphere at a heating rate of 1 °C min<sup>-1</sup>. GHMCSs was obtained from the thermally reduced composite film of GO and carbonized PF, while PS microspheres were removed and HMCs was simultaneously formed.

## 2.2 Exfoliation of graphite oxide

Exfoliation is among the four most common ways to fabricate graphene and can be broken down into many different types. The general method is carried out just as the title describes, it is the exfoliation of graphite layers. Mechanical exfoliation using scotch tape was the method used to fabricate the first ever sheet of graphene, but lacks the potential for large scale production within a time frame. A contradicting example consists of an economical method to produce high-quality graphene films similar to the scotch tape method in a large scale *via* a three-roll mill exfoliation.<sup>84</sup> One big difference with this study is the ability to continuously exfoliate graphite using the three-roll mill system, with the first and third drum rolling at the same direction and the second drum's rolling reversed. Rolling at a constant velocity, the rolled graphite will run in an inverted S curve. An adhesive was first prepared by dispersing 2.0 g of polyvinylchloride (PVC) into 50 mL of dioctylphthalate (DOP) in a magnetic stirrer at 250 °C for 30 minutes. The resulting adhesive was then carefully placed in between the feed and the

center of the rolls. 1.0 g of pre-dried natural graphite at 100 °C for 24 hours was carefully dispersed on the adhesive after the rolls started to move to attain maximum surface contact. After the exfoliation process has been carried out for 12 hours, the resulting materials was collected and steeped in alcohol to remove DOP from the product. After that, the sample was placed in a muffle furnace at 500 °C for 2 hours to burn away the PVC resin layer to obtain a purely graphene product.

One big problem with graphene is that graphene sheets tend to stack on top of each other, which causes a decrease in surface area. 2D and 3D porous graphene architectures were fabricated using KOH and CO<sub>2</sub> activation with EGO (exfoliated graphene oxide). All materials in this experiment were used without purification. GO was synthesized by a modified Hummers' method.<sup>85</sup> EGO was prepared by placing 1 g of dried GO in a quartz tube and purging with N<sub>2</sub> for a half hour to remove excess air. The tube was relocated to a vertical furnace at 800 °C for thermal exfoliation and was allowed to cool to room temperature under a N<sub>2</sub> flow. To create KOH-activated graphene, the chemical activation of EGO was used utilizing KOH as an activating agent. Dry EGO was mixed with deionized water and KOH was added. The mixture required 12 hours of stirring, and was then vacuum-dried at 65 °C. The resulting gray solid was then added to a crucible, where a N<sub>2</sub> glow was added to the tube for 1 hour to get rid of the air. Next, there would be a steady temperature increase to 800 °C. The product was then washed with deionized water, and then vacuum-dried marking the end of the KOH experiment. The product behaves differently based on the mass of KOH and EGO used. For the CO<sub>2</sub>-activated graphene, the process remained the same until the N<sub>2</sub> flow. After the N<sub>2</sub> stream, the temperature was increased and the gas stream was changed to CO<sub>2</sub> with no change of other variables. After CO<sub>2</sub> activation, it was cooled to room temperature under N<sub>2</sub>. The final product left a black spongy powder. The product was time dependent and not mass dependent. With fluctuation in the KOH/EGO mass ratio or in the time of CO<sub>2</sub> activation, activated graphene materials with a high specific surface area of 2518 m<sup>2</sup> g<sup>-1</sup> and a high specific capacitance of 261 F g<sup>-1</sup> would be obtained. Key factors that influence capacitance would include microporosity, specific surface, and surface wettability. A brief example of fabricating graphene using exfoliation paired with a template method for the use of capacitive deionization is as follows. Since chemical or thermal reduction of graphene exhibits lower electro-absorptive capacity from agglomeration, standard exfoliation was carried out to obtain graphene. The graphene was combined with microporous carbon (GE/MC) using a template method. This template method consists of a triblock copolymer F127 as a template and resol as a carbon precursor by a direct triblock-copolymer-template method. The resultant composites showed the mesoporous structure to be well structured with the addition of graphene. Specific surface area, pore size distribution, and pore volume were all improved through this method.<sup>13</sup>

In this example, the author discussed about interconnecting carbon fibers (CFs) in carbon cloth (CC) *via in situ* electrochemically exfoliated graphene. Carbon cloth are mechanically flexible woven carbon fibers, which are popular for their

electrical conductivity, flexibility, chemical stability and porosity. The issue presented on carbon cloth exhibits a very low surface area due to micro-sized gaps between the fibers during production. By interconnecting CFs, it showed significant amount of improvement in specific capacitance, surface area and conductivity.<sup>86</sup>

### 2.3 Chemical vapor deposition

Chemical vapor deposition (CVD) is a fabrication method used to produce high-quality thin film graphene, while maximizing its performance. It involves heating materials, in this case carbon, to a vapor and/or reducing the atmospheric pressure to coat a substrate. This substrate is a metal to act as a catalyst in the graphene growth.<sup>87</sup> It is the most commonly used fabrication method for graphene. The process is quite simple and has the potential to coat large surface areas. Electrochemical deposition, is also used for graphene fabrication, but is not nearly as commonly used since it may require a multi-electrode setup and because CVD is much more simple.<sup>88</sup>

This report described the production and fabrication methods used for devices that utilizes graphene, as well as the flexible electronic devices that are enabled by graphene.<sup>89</sup> Both chemical vapor deposition (CVD) combined with transfer techniques and chemical exfoliation (CE) have advantages for application on substrates like wafers, polymers, textiles, and even human skin. The CVD approach is known to grow large-area and high-quality graphene films using a carbon gas source. Common metals include Ni, Fe, Co, Pt, and Cu. To grow graphene film, there are 3 main stages: the diffusion of carbon into the metal film at a specific temperature, the stripping of carbon out of the thin metal film during the cooling process due to the reduction in solubility, and the formation of graphene layers on the surface. A relationship was found that a relatively high solubility of carbon atoms is projected to produce thick graphene films, as well as the other way around, having low solubility produce monolayer films. Other CVD methods like rapid thermal CVD method involves hydrogen-free, low-temperature conditions, which enables faster and larger production of films over a 400 mm × 300 mm surface area. Regardless of the method, substrate pre-treatments, polishing, and annealing are crucial for suppressing nucleation site density and even producing monolayer graphene. Another important factor for flexible electronic devices is graphene patterning techniques (direct patterned growth from a metal substrate). Another method called plasma enhanced chemical vapor deposition (PECVD) has benefits in contrast to CVD, like direct growth on a plastic substrate or nanostructures. However, CVD is still more effective, especially at high temperatures. This report includes more detailed methods and transfer methods.

An experimental example utilized a flexible transparent graphene electrode to improve the performance of perovskite solar cells due to the increase in demand to use perovskite solar cells as a reliable portable power source.<sup>4</sup> A CVD-grown graphene transfer method and copper foil was used to create a single layer graphene-deposited PEN substrates. The CVD grown single layer thick graphene film was deposited on the

copper foil, forming a graphene/copper foil composite. PMMA (poly(methylmethacrylate)) was spin coated on the graphene/copper foil composite and heated on a hot plate at 180 °C for 1 minute. The foil was then etched after placing it in an aqueous solution of ammonium persulfate ( $\text{H}_8\text{N}_2\text{O}_8\text{S}_2$ ). The resulting sample was placed on a UV-zone treated PEN-film and submerged in acetone solution to remove the PMMA. The graphene/PEN sample was then dried in a nitrogen blower. To increase the electrical contact, each sample of Cr, Au and Al was deposited consecutively through a rectangular metal aperture mask with a vacuum thermal evaporator. A  $\text{MoO}_3$  layer was deposited at a rate of 0.1 Å per s to adjust the surface properties. The sample was then annealed at 110 °C for 10 minutes and cleaned with acetone, isopropyl alcohol and deionized water for 15 minutes respectively, followed by UV-ozone treatment for 20 minutes. While during the whole fabrication process, it is crucial to maintain the flatness of the flexible substrate to ensure the properties of the highly efficient flexible solar cells. Glass/PDMS (polydimethylsiloxane) was used as a rigid support to achieve constant flatness. The graphene/PEN substrate or ITO was placed on the support for the whole duration of the fabrication process. Once the process was completed, the device was peeled off from the support to be characterized. Perovskite solar cells utilizing transparent graphene as a conducting anode produced a highly reliable and efficient results compared to the ITO counterparts.

Another research team looked into the utilization of graphene foam electrodes loaded with sulfur.<sup>90</sup> Generic Lithium Ion Batteries (LIBs) at its best were unable to meet high energy density and long life applications in the near future.<sup>91</sup> Although Lithium Sulphur batteries (LiS) was a strong contender for the next generation of batteries with much higher capacity and energy density with a two-electron reaction, sulfur loading in the cathode is inadequate.<sup>92</sup> Utilizing graphene foam ties the robust properties of graphene and porous network for high sulfur loading brings flexible Li-S battery electrodes. Ni foam grown graphene *via* CVD was reported in previous studies.<sup>93,94</sup> Briefly, the Ni foam was heated up in a horizontal tube furnace at 1000 °C with  $\text{H}_2$  atmosphere and annealed for 15 minutes to clean and eliminate the thin oxide layer on the surface.  $\text{CH}_4$ , with a concentration of 29 vol% in all total gas flow was introduced into the reaction tube with  $\text{H}_2$  and Ar at ambient room pressure for 30 minutes. Subsequently, the resulting sample was cooled to 100 degrees C  $\text{min}^{-1}$  under a Ar and  $\text{H}_2$  atmosphere. After the CVD growth process, a thin layer of graphene/poly(dimethylsiloxane) (PDMS) was coated onto the graphene surface on Ni foam by dipping it into a dilute PDMS solution for 30 minutes. The sample was then cured at 80 °C for 4 hours. The Ni substrate layer was etched away by placing it in a 3 M HCl solution at 80 °C for 12 hours to obtain PDMS/GF composite. A homogenous sulfur slurry was prepared by mixing sulfur and conductive carbon black at 10 wt% PVDF acting as a binder dissolved in *N*-methyl-2-pyrrolidone (NMP) to produce PDMS/GF electrode. The slurry was carefully cast into the PDMS/GF composite with a controlled sulfur loading to obtain the S-PDMS/GF electrode. The electrodes were ready to be used after drying it in a vacuum drying oven at 60 °C for 24 hours.

An example of a simple fabrication method consists of sandwich-like carbon nanotubes (CNTs)/NiCo<sub>2</sub>O<sub>4</sub> hybrid highly conductive paper.<sup>95</sup> The metal compound, spinel nickel cobaltite (NiCo<sub>2</sub>O<sub>4</sub>), exhibited ultra-high theoretical capacitance,<sup>96</sup> better electrical conductivity and variety of redox reactions.<sup>97</sup> NiCo<sub>2</sub>O<sub>4</sub> is also environmentally friendly and low cost and its natural abundance makes it very attractive for use in electrode applications.<sup>98</sup> Within the hybrid paper consist of a layer of conductive CNT buckypaper to house honeycomb-like NiCo<sub>2</sub>O<sub>4</sub> nanosheets and to provide strength that makes it flexible. A CVD method using ferrocene and dichlorobenzene as precursors was the method used to synthesize CNT buckypaper.<sup>99</sup> CNT buckypaper was sliced into approximately 0.9 × 0.7 cm<sup>2</sup> rectangular pieces and treated with UV/O<sub>3</sub> for 2 hours. Precursor solution was prepared by dissolving 4.17 mM Co(NO<sub>3</sub>)<sub>2</sub> · 6H<sub>2</sub>O, 2.06 mM Ni(NO<sub>3</sub>)<sub>2</sub> · 6H<sub>2</sub>O, and 6.25 mM urea in 30 mL methanol. A piece of as-prepared CNT buckypaper was placed into the precursor solution, followed by sealing the mixture in a 50 mL Teflon-lined autoclave. The mixture was hydrothermally treated at 120 °C for about 1 to 6 hours for the fabrication of the composites. After the sample was cooled, it was cleaned with deionized water repeatedly, followed by freeze-drying and annealed in air at 320 °C for 2 hours to obtain a CNTs/NiCo<sub>2</sub>O<sub>4</sub> paper-like electrode.

One report discussed about reduced graphene sheet (GR) patched carbon nanotubes (CNTs)/MnO<sub>2</sub> as a suitable pseudocapacitive electrode material as those materials which include a conductive polymer and transitional metal oxides has shown to have a much larger electrochemical capacitance and electrical densities.<sup>100–102</sup> MnO<sub>2</sub> alone possesses the characteristics of high-performance supercapacitors such as a wide potential range, environmental friendliness and low cost,<sup>103</sup> but lacks low conductivity and the flaking off phenomenon from the cyclic crystal shrinkage/expansion.<sup>104</sup> Multiwalled CNTs (MWCNTs) were first synthesized *via* Chemical Vapor Deposition (CVD). GO was obtained *via* Hummers' method and reduced to obtain a highly conductive GR nanosheet according to the literature.<sup>105</sup> The main process to obtain CNT papers was vacuum filtration. Catalyst particles was removed by carefully shearing MWCNTs to pieces (CNT cotton) with high speed shearing followed by immersing it into 5 mol L<sup>-1</sup> of aqueous hydrochloric acid solution for 48 hours. The cleaned MWCNTs were sheared the same way again and dispersed into deionized water this time *via* ultrasonic treatment with Tween-80 to act as the dispersant. Then, a cellulose filter membrane with a pore diameter of 0.45 microm was used to filter the uniformly dispersed CNT solution by vacuum filtration. The resulting sample was cleaned with deionized water several times to ensure the removal of remnant dispersants. The sample was placed and dissolved in acetone to obtain a freestanding CNT paper. The size of the CNT paper is controlled by the size of the filter, which ranges from 40 mm in diameter to A4 size. Electrochemical galvanostatic deposition with a two-electrode model was used to coat CNT papers with MnO<sub>2</sub> nanoparticles on the surface. For larger sized CNT papers, the papers were bent into a ring shape in a 500 mL graduated cylinder to act as the working electrode along with a stainless steel rod as the auxiliary electrode. The electrolytes

used in this process were 0.6 M MnSO<sub>4</sub> and 0.8 M H<sub>2</sub>SO<sub>4</sub>. The temperature of this whole process was controlled by a water bath. The composite paper was cleaned with deionized water to remove remnant electrolytes, then immersed in a 0.05 mg mL<sup>-1</sup> GR solution for a few hours to infuse the GR into the composite paper. The sample was then dried in a vacuum at 60 °C for 4 hours and collected to use. The counterpart of the asymmetric supercapacitor, flexible CNT/PANI composite paper was prepared with CV electrochemical polymerization in an electrolyte mixture that consist of 1 mol L<sup>-1</sup> H<sub>2</sub>SO<sub>4</sub> and 0.5 mol L<sup>-1</sup> aniline for 300 cycles. A saturated calomel (SCE) was used as the reference electrode and a graphite sheet was used as the auxiliary electrode. The voltage used in this process ranged from -0.2 V to 0.8 V with a scan rate of 100 mV s<sup>-1</sup>.

rGO/CNT is grown on Carbon Fiber (CF) with the combination processes electrophoretic reposition (EPD) of GO onto the surface of CF to follow up with floating catalyst chemical vapor deposition (FCCVD).<sup>106,107</sup> CNT is a great candidate to be utilized as the electrode material for supercapacitor fabrications.<sup>108–111</sup> To make the aforementioned samples, the CF-GO hybrid must be fabricated first. A plain-weave CF sheets (10 × 10 mm<sup>2</sup>) was acting as the substrate. 200 mg of GO was obtained from a modified Hummers' method with natural graphite powder.<sup>112</sup> The GO was dispersed into 100 mL of deionized water and sonicated for 1 hour. Then, CF sheets were connected to the positive and negative terminal of a constant voltage source. The CF sheets were soaked in GO solution with the voltage range of 2.0 to 5.0 V, with a deposition time of 1 minute. Next, the CF-rGO-CNT hybrid sample was fabricated. From the author's previous work,<sup>113</sup> CNT grafted CF-rGO was discussed. Briefly, a mixture of concentrated solution containing carbon source/catalyst was prepared. 0.35 g of ground ferrocene was dissolved into 7 mL of xylene solution and sonicated for 1 hour until the color turned orange red. Then, the CF-GO hybrid was placed in the middle of the furnace under 200 scum argon atmosphere through a tube furnace to ensure no air was left in the system. The furnace temperature was set to 750 °C at the heating rate of 15 °C min<sup>-1</sup>, with 50 scum hydrogen and 350 scum argon. The final mixture was injected into the furnace with a rate of 0.2 mL min<sup>-1</sup> for 30 minutes and an additional 5 minutes for reaction. The final product obtained was the CF-rGO hybrid that can be directly used as a template for CNT growth. CF-rGO-CNT hybrid growth can be seen in Fig. 8.

## 2.4 Epitaxial growth

Epitaxial growth is a fabrication method used to produce large scale graphene films as a microfabrication process. It can be grown and can incorporate CVD as a process to deposit graphene on specific substrates. When deposition is involved the main difference between the two is that CVD uses conducting substrates while epitaxy uses an insulator substrate.<sup>114</sup> Epitaxial growth is known to use SiC because of its flexibility and carbon content so that when the silicon is removed or melted, carbon (graphene) can be left over depending on how the experiment is carried out. Different commonly used ways of measurement for characterization include STM and LEEM. Fabricating graphene

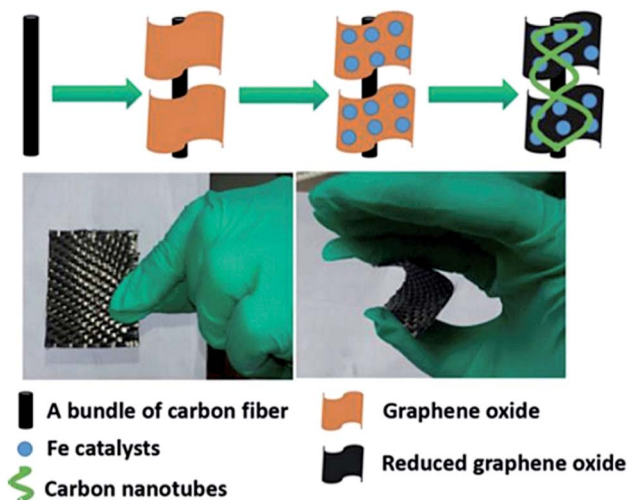


Fig. 8 Schematic of the fabrication procedure to produce the CF-rGO-CNT hybrid. Inset picture shows the before and after CNT growth effects on the CF-rGO substrates.<sup>106</sup>

through epitaxial growth is a great option for large-scale application-fitting desires, but a uniform thickness on a large domain remains a difficulty to get past, along with substrate bonding affecting the electronic properties of the graphene layers produced. The use of different substrates allows for eliminating these drawbacks. For example, one source sets out to use epitaxial growth on ruthenium(0001) to produce arrays of graphene in a layer-by-layer fashion to provide a path towards synthesis for applications in electronics.<sup>115</sup>

Because of graphene's properties, creating N-doped graphene for electrode material in recent studies show that N incorporation in graphene can potentially enhance the electron transfer efficiency for use in electrochemical capacitors. In this experiment, graphene nanowalls (GNWs) and N-doped graphene nanowalls were synthesized on a carbon cloth (CC). Before the synthesis, the CC was brought into a MPECVD chamber. H<sub>2</sub> plasma was ignited by supplying 99.999% H<sub>2</sub> into the chamber to get rid of impurities from the CC at 900 degrees

celsius, 40 Torr, and 1500 W for a few minutes. Once H<sub>2</sub>, CH<sub>4</sub>, and SiH<sub>4</sub> (200 : 5 : 1) were added in, plasma was maintained under 1500–2000 W at 1300 degrees celsius for a few hours to allow SiC nanowalls to grow. The supply of CH<sub>4</sub> and SiH<sub>4</sub> was stopped while the substrate temperature was kept at the same temperature. The layers of graphene were grown covering the SiC nanowalls from surface graphitization under H<sub>2</sub> plasma ambient within seconds. The GNWs were functionalized within NH<sub>3</sub> by prolonging the process soon after the end of CH<sub>4</sub> and SiH<sub>4</sub>, which is the N-doping. The process describes successful large-scale direct-growth for GNWs on a flexible substrate. The result NGNW showed maximum specific capacitance of 991.6 F g<sup>-1</sup>, an energy density of 275.4 W h kg<sup>-1</sup>, and a power density of 14.8 kW kg<sup>-1</sup>.<sup>116</sup>

Another team of researchers presented a low-cost and simple epitaxial lift-off flexible and transparent single-crystal gold foil electrodes with silicone as the base.<sup>117</sup> The interest is to move beyond the conventional silicone-based chips to innovate newer electronics such as flexible transparent displays, wearable solar cells, and sensors.<sup>118–123</sup> Although numerous breakthroughs with ultrathin Si foils were found to support flexible devices and architectures, the typical fabrication process for ultrathin Si foils, vacuum evaporation or sputtering, are known to suffer from polycrystallinity or textured deposit that leads to electron-hole recombination at grain boundaries.<sup>124</sup> This research presented a wafer-sized flexible and transparent gold foils. With the help of the epitaxial lift-off method on single-crystal substrates, a free-standing single-crystal foils can be fabricated by dissolving an adhesion layer as the sacrifice.<sup>125</sup> An epitaxial lift-off procedure for ultrathin electrodeposited Au single crystal foils on the Si(111) substrate was shown in Fig. 9. A method developed by Allongue and co-workers were used to electrodeposit epitaxial Au on the Si(111) substrate.<sup>126,127</sup> A single-crystal Si(111) with properties such as 1.15 ohm cm of resistivity and 0.2° miscut towards<sup>112</sup> was used as the substrate for Au foil growth. 0.1 mM HAuCl<sub>4</sub>, 1 mM KCl, 1 mM H<sub>2</sub>SO<sub>4</sub>, and 0.1 M K<sub>2</sub>SO<sub>4</sub> with a pre-polarized Si electrode at -1.9 potential voltage vs. Ag/AgCl was inserted into the solution to perform the deposition process at room temperature. The pre-polarization

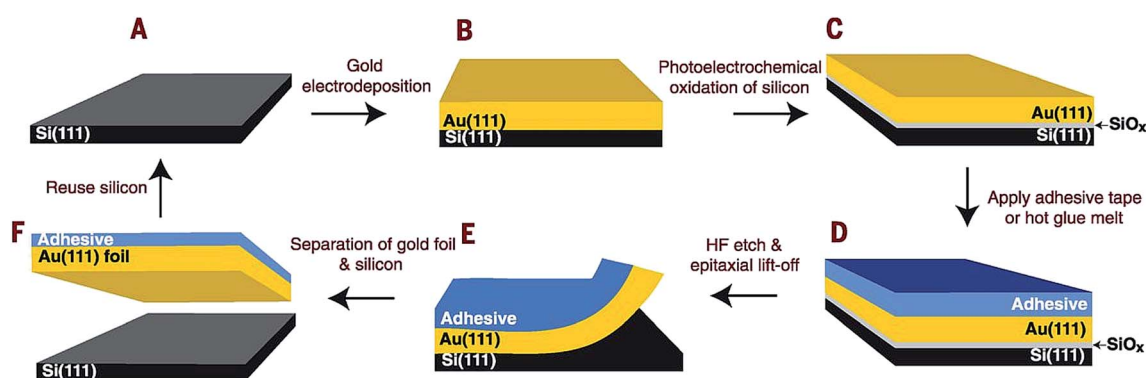


Fig. 9 Depiction of the epitaxial lift-off method on a single-crystal Au foil. (A) A pure n-type Si(111) non-oxidized wafer. (B) Epitaxial deposition of Au on the Si(111) wafer. (C) An inset of SiO<sub>x</sub> layer in between the Au and Si layer via photoelectrochemical oxidation of Si under irradiation of light. (D) A form of adhesive (tape/hot glue) was placed on the Au layer to assist in the lift-off process. (E) Sacrificial SiO<sub>x</sub> layer was etched to provide easy separation of the Au foil from the Si substrate. (F) A successful separation of the Au foil from the Si substrate.<sup>117</sup>

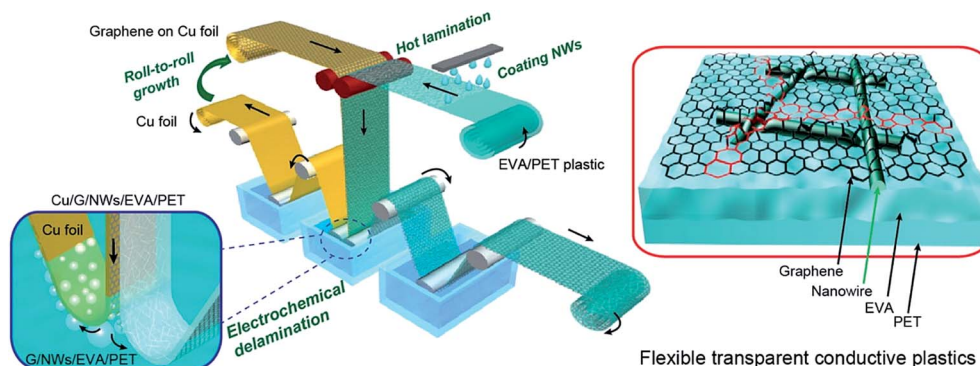


Fig. 10 Roll-to-roll process involving the growth stage, hot lamination, NW coating, and electrochemical delamination.<sup>140</sup>

of the electrode activated the epitaxial growth of Au and helped with the formation of an amorphous native oxide layer on the substrate. A sacrificial  $\text{SiO}_x$  layer was grown in between Au and Si deposits *via* photoelectrochemically oxidizing Si under 0.75 potential voltage of light irradiation *vs.* Ag/AgCl in 0.5 M  $\text{H}_2\text{SO}_4$  solution. Then, a polymer adhesive as the additional support and facilitator for the foil separation process was added onto the surface of Au. The etching process was carried out by using 5% dilute hydrofluoric acid to detach Au foil from the Si substrate. The foil was easily separated from the etched  $\text{SiO}_x$  layer. The remaining Si substrates were etched with 0.6 M of KI and 0.1 M of  $\text{I}_2$  solution to dissolve any Au particles to ensure a clean Si substrate ready to be reused. The Si substrate can be reused numerous times because each removal process of the 2–3 nm thick  $\text{SiO}_x$  during fabrication was without extensive roughening (Fig. 10).

## 2.5 Quality enhancement techniques

Quality enhancement techniques are done within an experiment to assist the main methods that were earlier described. One or all methods can be involved within an experiment and each offers results that make fabrication more successful or simpler. A compiled set of advantages and disadvantages of using each enhancement factor can be found in Tables 2 and 3. Other techniques can be implemented and created in fabrication, like using a Fe-catalyzed glucose-blowing approach with  $\text{NH}_4\text{Cl}$  as a blowing agent and Fe as a graphitization catalyst to fabricate graphene-like carbon nanosheets.<sup>134</sup> Even doping graphene with dual atom (N, P) will significantly boost the

oxygen reduction reaction (ORR) and the oxygen evolution reaction (OER) performance.<sup>135</sup>

**2.5.1 Vacuum filtration.** Suction (vacuum) filtration is a technique carried out in chemistry recrystallization experiments that gives a greater rate of filtration. Compared to normal filtration, which uses gravity as the force to push the liquid through the filter, vacuum filtration uses a pressure gradient. This allows for a variable rate depending on the pump strength. Vacuum filtration can be applied to any method, since its effects can benefit GO substitutes or solutions in different ways. It can also be implemented in ways to insert nanostructures within graphene sheets, like the example of a filtration method *via* self-assembly of water dispersible graphene and mesoporous carbon nanosphere (MCS) using the MCS to be inserted between graphene sheets by vacuum filtration.<sup>136</sup> Overall, it is done to filter out liquid in a solution so that all that is left is graphene.

To reproducibly obtain uniform thin films with enough GO layers over large surface areas, the vacuum filtration method is a good approach. The vacuum filtration method can be used widely to deposit highly uniform single-walled carbon nanotube thin films. As described in the following experiment, as well as in a general sense, vacuum filtration is the filtration of a GO suspension through a commercial mixed cellulose ester membrane, which has an average pore size of 25 nm.<sup>137</sup> The membrane pore sizes can vary for each experiment depending on the desired filtration. The liquid passes through the pores, but the GO sheets become lodged.

Another report starts out with GO from applying the modified Hummers' method.<sup>17</sup> In preparing the rGO films, vacuum

Table 2 Pros and cons of discussed methods

Method	Pros	Cons	Citations
General Hummers' method	Quick oxidation method, most effective	High consumption of oxidants and intercalating agents	17 and 128
Exfoliation of graphite oxide	Simplicity, low cost	High cost and poor scalability in real-world applications	84 and 85
Chemical vapor deposition	Large quantity, high quality, single layer graphene (SLG)	Hard to fabricate on a large scale	18, 38 and 129–132
Epitaxial growth	Large quantity, van der Waals heterostructure	Expensive equipment, time consuming	115 and 133
		High temperature, inconsistent uniformity, effects of substrate bonding	

filtration was applied to aqueous solutions of the created GO using mixed cellulose ester membranes as the filter (filtration volume can fluctuate depending on the desired film thickness and transparency. This also applies to variance in GO solution concentration). Here it can be seen that transparency and film thickness are key elements in vacuum filtration, along with the pump strength to determine the variable rate of flow.

In an example of a hybrid fabrication method, one team compared the use of carbon black (CB) as a conductive additive for both graphene and reduced graphene oxide (rGO).<sup>138</sup> The graphene/CB mixture acts as a good supercapacitor electrode. The reduced graphene oxide/CB mixture was subjected to vacuum filtration methods to obtain a free-standing, flexible nanocomposite film. Vacuum filtration is essential in obtaining the film, regardless if it is a hybrid material or not. The benefit of using CB is that it not only acts as a conductive additive but it also acts as a spacer which prevents restacking of rGO layers. Preventing restacking is desirable because it means that the layer(s) will reach a larger surface area and higher capacitance. CB amounts must be balanced/regulated though, because too much can cause agglomeration.

**2.5.2 Roll-to-roll production.** Roll-to-roll (R2R) production is a unique complementary method and transfer process that falls under CVD. It involves a multistep process with a long and thin copper film for the graphene to be applied to. Roll-to-roll production is usually accompanied by wet-chemical doping of (mainly) monolayer graphene films grown by chemical vapor deposition onto flexible copper films.<sup>139</sup> Due to lack of efficient methods for synthesis, transfer, and doping of graphene at the nanoscale, the production of transparent conducting films from graphene are difficult. In the roll-to-roll wet chemical doping process, there are essential steps to ensure success. The films used have sheet low resistances ( $\sim 125$  ohms) and high optical transmittance ( $\sim 97.4\%$ ). The graphene film was grown on copper foil and attached to a thin adhesive polymer film. Copper was removed by electrochemical reaction with a solution; in the following case it was ammonium sulfate. Finally, the films were separated so that the graphene film can be thermally treated. It is assumed that the graphene was grown on copper foil because of its relatively cheap price point and electrical conductivity. Copper foils with larger grain size yielded higher-quality graphene films. The copper foils were heat-treated to increase the grain size.

An in-depth experimental detail showed a similar approach and explained their four key steps for the R2R encapsulation.<sup>140</sup>

The first step was R2R growth of a long monolayer graphene film on Cu foil from the CVD method. Second was either coating or transfer of metal nanowires onto a EVA/PET (ethylene vinyl acetate/polyethylene terephthalate) plastic film. The usage of the exact plastic as the film in other experiments was optional. Third, hot lamination of graphene/copper foil onto metal nanowires precoated with EVA/PET plastic was carried out. Finally, electrochemical bubbling delamination of graphene film from copper foil was done. The process started out with a roll of continuous monolayer graphene film grown on  $5\text{ cm} \times 5\text{ m}$  copper foil by the CVD method. After electrochemical transfer, Cu foil could be preserved and reused for graphene growth. The following figure illustrates the process that is being described (Fig. 11).

Three cycles were conducted and after Raman spectra analysis, the graphene R2R grown on the reused copper foil was improved. This was from the surface flattening and grain size enlargement of the foil during high temperature annealing. Next, the metal nanowires were coated on the EVA/PET sheet by using a Mayer rod. The EVA surface was pretreated by air plasma so that its hydrophilicity is improved. Once the CuNWs (copper nanowires) were coated, Cu/graphene film was hot-laminated onto the CuNWs which creates a laminated structure at 100 degrees C. This was done by two rollers giving off the specified heat and mechanical pressure during the lamination. This process reduced air traps, cracks, or any blemishes due to the simultaneous heat and pressure. What was left was a cathode film of Cu/graphene/NWs/EVA/PET. Finally, it was stripped away of the lamination by, what the source calls it, the electrochemical bubbling delamination transfer method. This process involved the laminated film to be partially immersed in water. While immersed, hydrogen bubbles were generated through water electrolysis, which delaminated the graphene film at a very low electrolysis voltage. The speed at which the film immersed and emerged can reach up to  $2\text{ cm s}^{-1}$ . Since the cathode has a negative charge during the delamination process, the films can avoid oxidation and the Cu foil can be reused. The resulting graphene/NW/plastic films proved to have high optoelectronic performance, great corrosion resistance, flexible, and adhesiveness. This film proved to be successful for flexible, transparent electrodes. It offered mass production and low cost, which helped pave a pathway to future applications. Other R2R experiments may include alterations like expanding the length of the copper foil to 100 meters long in the process.<sup>130</sup> Another group fabricates films at 294 mm thin under low

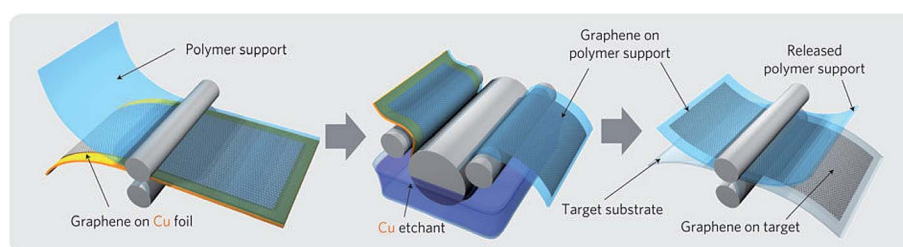


Fig. 11 In depth illustration on the roll-to-roll producing graphene films on a copper film involving adhesion of polymer supports, Cu etching and dry transfer printing.<sup>139</sup>

temperatures.<sup>131</sup> This shows that the R2R complementary factor does not have to be done in critically specific ways. However, the experiment provided by Deng and Hsu does provide an appropriate film length and appropriate steps to fabricate a stable, successful electrode (Fig. 12).

**2.5.3 Ultrasonication.** Ultrasonication is a process that applies sound energy to agitate particles in a sample with frequencies greater than 20 kHz. It reduces small particles in a liquid to enhance stability and uniformity. Two common ways to apply ultrasonication to a solution are by bath and probe units. Even though bath units are more commonly used, they have two drawbacks that decrease experimental repeatability and reproducibility.<sup>141</sup> These two drawbacks are a lack of uniformity and a decline of power over time. A lack of uniformity is resulted from ultrasonic baths because only a portion of the volume of the ultrasound source experiences cavitation. Luque-Garcia and De Castro suggested that ultrasonic probes have the upper hand over ultrasonic baths since they focus their energy on a localized sample zone, which allows for more efficient cavitation (Fig. 13).

This experiment started out by using Hummers' method to oxidize and form the graphite oxide.<sup>132</sup> It was then added to a concentrated solution of  $\text{H}_2\text{SO}_4$ ,  $\text{K}_2\text{S}_2\text{O}_8$ , and  $\text{P}_2\text{O}_5$  with an atmospheric temperature of 80 degrees C. Further experimental processes similar to the Hummers' method examples were carried out until the point that the obtained graphite oxide powder was dried and dialyzed in 0.5% graphite oxide dispersion. At this point, a new approach was taken instead of the common next step of exfoliation of graphite oxide. SDBS (sodium dodecylbenzene sulfonate) was added as a surfactant, which facilitated the exfoliation, lowered the surface tension, and allowed for a larger sheet of graphene oxide from ultrasonication. Using ultrasonication as the exfoliation method allowed for particle agitation to properly exfoliate the solution. It is typical to sonicate  $0.1 \text{ mg mL}^{-1}$  graphite. In a review, sonication was carried out with lithium salt intercalated

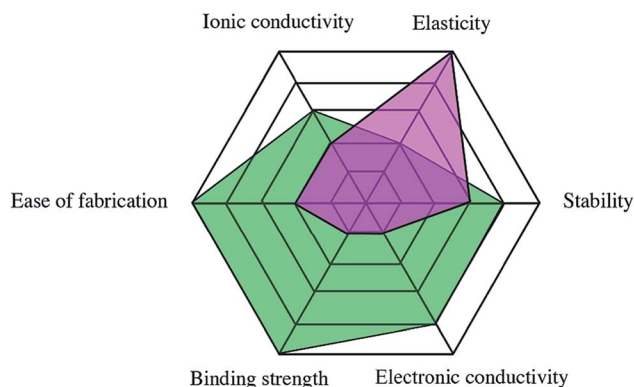


Fig. 13 Comparison of cellulose paper (green) and polymer non-conductive substrates (purple) for flexible electrodes (conductive meaning graphene).<sup>163</sup>

graphite mixed with water.<sup>142</sup> It recorded more than 80% few-layer graphene, where lithium and water react to form hydrogen gas which can further aid exfoliation (Fig. 14).

One group utilized fibers as the base for a superconductor material that was capable of showing great performance in conductivity and capacitance.<sup>143</sup> A flexible fiber-shaped supercapacitor (FSSCs) was recently picked up by researchers due to its potential to be assembled into other structural systems in flexible electronic applications for its tiny volumes, structural flexibility, and high capacitance density.<sup>144–148</sup> The ED (electronic deposition) method was previously reported to prepare the nickel-coated CF (carbon fiber) successfully.<sup>149</sup> The fabrication of nickel-coated carbon fiber started off treating CF threads with acetone, alcohol and distilled water respectively under ultrasonication for 15 minutes. After that, the CF thread was immersed in  $10 \text{ g L}^{-1}$  of  $\text{SnCl}_2$  for 20 minutes, followed by cleaning it with distilled water several times and then drying it at  $70 \text{ C}$ . Subsequently, the CF thread was immersed into  $0.25 \text{ g L}^{-1}$  of activated  $\text{PdCl}_2$  and  $10 \text{ mL L}^{-1}$  of hydrochloric acid

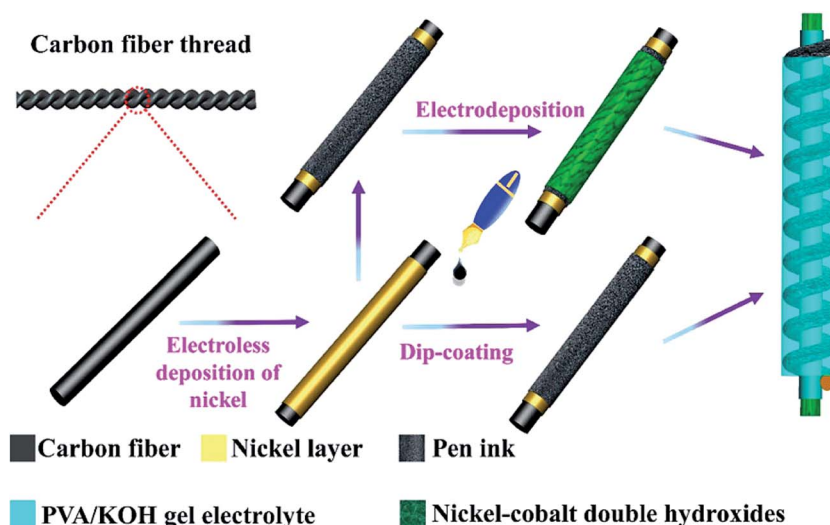


Fig. 12 Illustration of the fabrication process to produce flexible fiber-type solid-state asymmetric supercapacitors.<sup>145</sup>

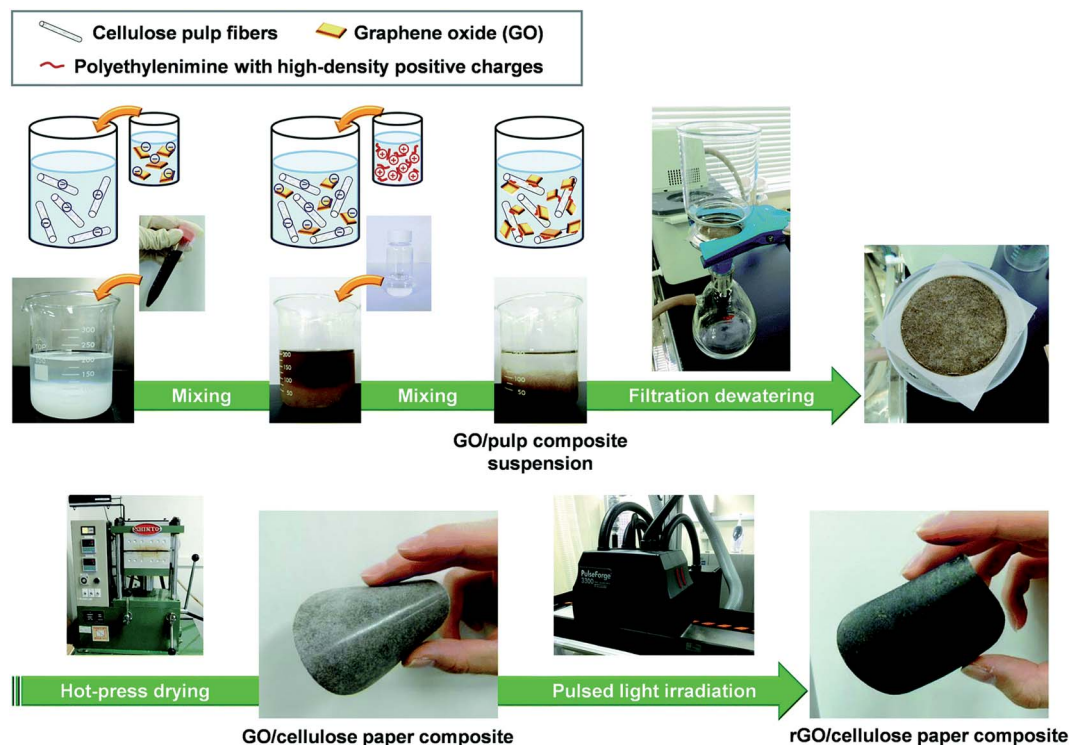


Fig. 14 Depiction of the preparation procedure for the rGO/cellulose paper composite via papermaking and successive flash-reduction processes with a paper composite thickness of 100  $\mu\text{m}$  and diameter of 75 mm.<sup>171</sup>

solution for 20 minutes, then the same cleaning and drying process as before was repeated. The resulting treated CF thread was then immersed into a homemade plating bath (40 g L<sup>-1</sup> of NiSO<sub>4</sub>·5H<sub>2</sub>O, 20 g L<sup>-1</sup> of sodium citrate, 10 g L<sup>-1</sup> of lactic acid and 1 g L<sup>-1</sup> of dimethylamine borane in water) at 90 °C for 15 minutes to undergo an electronic deposition method to obtain the metallic structure in the water bath. The next step is to fabricate the pen ink/nickel/CF via facile dip-coating method.<sup>150</sup> The procedure required the previously prepared nickel-coated CF to be immersed into pen ink solution (average thickness of in film = 600 nm) for 5 minutes. After that, the nickel/CF was transferred into a hot stage at 60 °C for 2 hours. The desired thickness of pen ink to be coated on nickel/CF could be controlled via repeating the aforementioned process until desired thickness was obtained. Then, the fabricated pen ink/nickel/CF sheet was coated with Ni-Co DHs via ED method in a standard three-electrode system at 25 °C. The pen ink/nickel/CF was treated as the working electrode, where else a Pt wire was the counter electrode and the saturated calomel electrode (SCE) as the reference electrode. 100 mL of 0.1 M metal ion solution with Ni<sup>2+</sup>/Co<sup>2+</sup> with a 1 : 2 ratio was the acting electrolyte for the process, with the voltage range from -1.0 V for 10 minutes. The resulting Ni-Co DHs/pen ink/nickel/CF sheet was cleaned with distilled water followed by drying at 60 °C for 30 minutes. The final process involved the assembly of solid fiber supercapacitor. An electrolyte consisting of PVA/KOH gel was prepared with 3 g of dissolved PVA in 20 mL of distilled water at 100 °C under vigorous stirring for 1 hour. Subsequently, 10 mL

of 0.3 g mL<sup>-1</sup> KOH solution was added into the previous mixture via the drop method gradually, followed by a continuous stirring at 80 °C for 1 hour. Then, Ni-Co DHs/pen ink/nickel/CF was used as the positive electrode while pen ink/nickel/CF was used as the negative electrode for the ED process consisting of the prepared gel electrolyte for 5 minutes. After the ED process, the resulting samples were taken out to be dried at room temperature. Finally, PVA/KOH gel electrolyte was used to assemble the previously said electrode together, placed in a silicone tube to be protected and heated at 60 °C for 2 hours to evaporate excess water contained in the electrolyte.

**2.5.4 Hydrothermal.** The hydrothermal method is a method used for substances that are intended to be mixed with graphene to create a hybrid. This method involves using an autoclave and temperature control to crystallize or recrystallize a substance. It can also apply to any main method of fabrication, since the hydrothermal method allows for crystallization and each method can operate with a solid hybrid material. In the following example, fabrication of a graphene/vanadium hybrid supercapacitor electrode took place. The mixtures were designated as VURGO and VSRGO (Vanadium Ultralarge/Small Reduced Graphene Oxide) and were produced through the following process.<sup>151</sup>

The preparation of UGO started with thermally expanding graphite flakes and synthesizing GO using Hummers' method. The GO was diluted with deionized water and centrifuged at 8000 rpm for 40 min, which was when the SGO was obtained. The sediment was spread in deionized water and centrifuged



another time, except at 4000 rpm. A precipitate was produced, which contained the UGO, and was added to DI water. Usually, ultrasonication is a step that follows this, but it was not done here specifically because it reduces the lateral size of the GO sheets. The highest yield for UGO was at 8.3 wt%. Modifications should be made to see a higher yield for UGO.

In continuing to fabricate VUGO and VSGO, the  $\text{VO}_2$  was synthesized by the hydrothermal method, which crystallized the substance for high-quality crystal growth and composition control. Using a  $\text{VO}_2$  : UGO weight ratio of 7.3 or using an annealing temperature of 250 °C for 2 hours are two ways to optimize the electrodes in forming a free-standing film. The VUGO mixture was stirred at 70 °C for an hour and then filtered through a cellulose acetate membrane by a method of vacuum filtration. Make it known that the transparency and film thickness will depend on the characterizations of the membrane used. The film must be washed with DI and dried several times until it can be removed from the filter paper. The film was annealed at 250 °C for 2 hours in argon gas so that the GO could change to reduced graphene oxide (rGO). VURGO showed better results than VSRGO because of its porosity and interconnected structure. This example showed that the hydrothermal method used to fabricate a graphene mixture can simply apply to just the hybrid material being added (in this case the  $\text{VO}_2$ ).

One group discussed about a freestanding reduced graphene electrode coated with carbon  $\text{Li}_4\text{Ti}_5\text{O}_{12}$  nanosheets (LTO-C/rGO) to be used in sodium ion batteries.<sup>152</sup> The electrochemical performance of nano/microstructured LTO composites and carbon-based materials such as CNT and graphene was focused to be improved. Carbon nanotubes shortens both electron and Na ion transport lengths,<sup>153–155</sup> where else graphene provides more efficient electron transportation.<sup>156–161</sup> First, a modified hydrothermal method with annealing was used to fabricate LTO nanosheets.<sup>162</sup> The process involved 1.7 mL (5 mM) of tetrabutyl titanate, 0.189 g of  $\text{LiOH} \cdot \text{H}_2\text{O}$  and an estimated amount of  $\text{GdCl}_3 \cdot 6\text{H}_2\text{O}$  mixed into 20 mL of ethanol under magnetic stirring for 24 hours at room temperature. After that, 25 mL of deionized water was added into the mixture and stirred for 0.5 hours. The resulting solution was then transferred into a 50 mL Teflon-lined stainless autoclave and placed into an oven. The solution was heated to 180 °C for 36 hours to achieve  $\text{Li}_{1.81}\text{H}_{0.19}\text{Ti}_2\text{O}_5 \cdot x\text{H}_2\text{O}$  (H-LTO). After the hydrothermal process, a white H-LTO precursor was collected

at the bottom of the reactor. The aforementioned sample was then washed with ethanol 3 times, followed by heating at 700 °C for 6 hours in a horizontal furnace tube with air to get LTO nanosheets. Next, LTO nanosheets needed to be coated with carbon. H-LTO precursor was then prepared and allocated 200 mg to be dispersed in 10 mL of ethanol under magnetic stirring. Nominal 5 wt% of H-LTO precursor and D(t)-glucose ethanol was dissolved in 5 mL of ethanol and later to be dropwise added into the previous solution and stirred, followed by slow evaporation at 80 C. The resultant slurry was heated to 700 °C under stirring with Ar/ $\text{H}_2$  (5%) atmosphere for 6 hours to obtain carbon-coated LTO (LTO-C) nanosheets. The final step was to obtain LTO-C/rGO film by getting GO *via* oxidized graphene using modified Hummers' method. LTO-C nanosheets were dispersed into 100 mL of 1 M  $\text{NH}_4\text{HCO}_3$ , later to be added drop-wise into a solution with dispersed GO in 100 mL of deionized water with magnetic stirring. The resulting black composite that sank to the bottom within 10 minutes was collected with vacuum filtration through a microporous filter (0.45 microm). The black composite was dried at 60 °C for 6 hours, then peeled off and annealed at 700 °C under an Ar/ $\text{H}_2$  (5%) atmosphere for 2 hours. Then, a free-standing LTO-C/rGO film was fabricated.

**2.5.5 Substrates.** There are two main types of bendable electrodes for LIBs/SCs. One uses nonconductive bendable substrates, such as paper, polymers, and textiles to support the active materials.<sup>163–166</sup> The selected materials must meet certain requirements including ability to deform under stress/strain. The other uses conductive supports, which involve CNTs or graphene films with high conductivity. On top of having an ideal elastic modulus and having ionic conductivity, whatever material used for the flexible electrode (in this case graphene) should have substrates that do not produce any contaminants during electrochemical reactions and should be totally inactive against any chemicals in the system. High resistances would be a drawback too. Polymer substrates have high resistances, which acts against what is trying to be achieved, so the use of substrates with lower resistances like Cu or Al foil current collectors is more desirable. The figure below shows the difference between using polymer substrates (purple) and using cellulose paper/cloth substrates (green).

**2.5.6 Comparison table for quality enhancement techniques.**

Table 3 A comparison table for quality enhancement techniques

Methods	Pros	Cons	References
Vacuum filtration	Large surface area (Eda)	Cost of equipment, time	17
Ultrasonication	Stability and uniformity	Reduce lateral size of graphene	151
Hydrothermal	Nanometer sized graphene sheets, for hybrid materials	Long hours required	151 and 167
Substrates	Can optimize properties	Poor selection can result in lack of properties	163 and 167
General environmental methods	Utilizing recyclable materials	Time, money, does not yield the best characteristics	4, 168 and 169

### 3 Environmental impact and toxicity

While each fabrication method conveys desirable results, some methods do have environmental drawbacks. For example, in Hummers' method, due to  $\text{NO}_2$  and  $\text{N}_2\text{O}_4$ , toxic gas can be generated. Other drawbacks include residual nitrate and low yield. Many attempts have been made to modify this method like replacing the  $\text{NaNO}_3$  or adding a peroxidation step before the  $\text{KMnO}_4$  oxidation.<sup>14</sup> Overall, there is a high demand for an economic, cost-effective, environmentally friendly process to synthesize GO. The researchers tackle these problems to make a modified Hummers' method more desirable for practical application. When increasing the amount of  $\text{KMnO}_4$  and concentrated  $\text{H}_2\text{SO}_4$  (with  $1/9 \text{ H}_3\text{PO}_4$ ) in place of  $\text{NaNO}_3$ , the modified Hummers' method leads to higher yield, easier temperature control, and less toxicity.

On the renewable/recyclable side, a proposal came up to recycle industrial waste and utilize it as graphene electrodes using coal tar pitch (CTP) as carbon feedstock.<sup>170</sup> Dilute coal tar pitch with 8 wt% of quinoline solvent was used. Then the mixture was spin coated at 6000 rpm for 1 minute on a  $\text{SiO}_2$  (500 nm)/Si substrates and baked at  $240^\circ\text{C}$  for 30 minutes. The next step was to deposit the Ni layer (200 nm) on a coal tar pitch film at room temperature (Magnetron Sputtering System, SNTEK; working pressure 7 mTorr; power 50 W; Ar flow rate 50 sccm). The resultant film was then annealed using a thermal CVD method at  $1100^\circ\text{C}$  for 4 minutes with flowing 50 sccm of Ar and 10 sccm of  $\text{H}_2$ , with a combined pressure at 0.3 Torr. Then, the tube was removed from the furnace but maintained the same amount of Ar/ $\text{H}_2$  flow to cool the film to room temperature. Once cooled, the Ni layer could be etched away and cleaned with deionized water after dipping the sample film into  $\text{FeCl}_3$  solution for 1 minute (iron(III) chloride solution  $45^\circ\text{Be}$ ).

The process to get a flexible electrode is time consuming and tedious, usually involving high-temperature treatment or the use of toxic chemical treatment.<sup>171</sup> Hence, the researchers showed a method that can be fast, scalable and environmentally friendly to fabricate a high-performance rGO/cellulose paper supercapacitor electrode. An aqueous suspension of cellulose pulp fibers that consist of virgin pulps and recycled waste pulps from newspapers (0.15 wt%, 200 mL) was mixed with aqueous dispersion of single layer GO sheets that was purchased ( $\text{GO}_0\text{TQ}_2$ , 1 wt%, width: 10–30  $\mu\text{m}$ ) (0.032 wt%, 15.5 mL, GO content: 5 mg) and an aqueous solution of poly-ethylenimine (PEI) (average molecular weight: 1800) (1.0 wt%, 0.4 mL) with intervals of 10 minutes in between adding each solution. The resultant solution was then filtered by suction filtration through a #300 wire mesh for 4 s. After that, the wet paper sample was sandwiched between a hydro-phobic glass and paper towel followed by hot pressing it at  $110^\circ\text{C}$  for 10 minutes to dry the sample (1.1 MPa). The resultant sample was then peeled off from the wire mesh to make a GO/cellulose paper composite with a diameter of 75 mm and a thickness of ca. 100  $\mu\text{m}$ . The GO/cellulose paper then underwent flash reduction at room temperature in air using a Pulse-Force 3300 equipped with xenon flash lamps. The process was carried out

10 times at a frequency of 2 Hz for each surface of the GO/cellulose paper composite.

To obtain reduced graphene oxide, a general method is to use a reducing agent to chemically reduce GO to rGO. Reducing agents usually possess harmful characteristics such as toxicity, flammable and reactivity. A way to harness the aqueous extract of *Hibiscus sabdariffa* L. was figured out<sup>172</sup> to be used as a reducing agent, which in contrast, non-toxic and significantly cheaper. To make GO, a modified Hummers' method was used. 1.0 g of natural graphite sheets was gathered and added into 100 mL of concentrated sulfuric acid ( $\text{H}_2\text{SO}_4$ ) while stirring it for 1 hour in an ice bath. After that, 4.0 g of potassium permanganate ( $\text{KMnO}_4$ ) was slowly added into the solution in a water bath at room temperature for 6 hours. 200 mL of deionized water was then added to dilute the solution followed by adding 100 mL of deionized water and 20 mL of hydrogen peroxide ( $\text{H}_2\text{O}_2$ ) into the solution gradually while stirring. The solution eventually changed color from dark purple to a bright yellow brown solution. The stirring solution was allowed to rest at room temperature for 24 hours. After 24 hours, the solution was then centrifuged and cleaned with deionized water until the pH level is neutral, followed by drying the sample in a vacuum pumping system at room temperature. Next, preparation of the aqueous extract of *Hibiscus sabdariffa* L. was executed by purchasing 10.0 g of *Hibiscus sabdariffa* L. and adding it into 1.0 L of deionized water. The mixture was then heated to  $60^\circ\text{C}$  for 1 hour. The resulting aqueous extract then could be obtained by filtering the solution using 0.45  $\mu\text{m}$  pore size polypropylene filter papers. To reduce GO, 80 mg of GO suspension was put into 200 mL of *Hibiscus sabdariffa* L. aqueous extract. The mixture was then subjected to ultrasonication for 1 hour and followed by subsequent stirring and heating for another hour. After that, the sample was cleaned with deionized water and vacuum dried at room temperature. To get a flexible graphene film electrode, HRGO-R in 0.4 mg  $\text{mL}^{-1}$  of deionized water had to be dispersed under ultrasonication followed by filtration and drying at  $70^\circ\text{C}$ . Graphene films could be obtained by peeling off 1  $\mu\text{m}$  of HRGO-R. Supercapacitors could also be created by placing two graphene films separated by a filter paper soaked with 1 M  $\text{H}_2\text{SO}_4$  that acted as the electrolyte. Then placing two platinum foils acting as a current collector in a sandwich-like structure formed the supercapacitor cell.

This source showcases an eco-friendly fabrication method of a 3D porous structured aerogel that encapsulates characteristics like large specific area, efficient ion-diffusion, superior mechanical integrity and multidimensional continuous pathways for electron transport for high performance energy storage and conversion applications, catalysis and adsorbents for environmental remediation.<sup>173–175</sup> The most common method to fabricate graphene hydrogels in the research field seems to be *via* hydrothermal method.<sup>176–178</sup> The simple fabrication process allows significant savings in industrial terms to produce high-performance electrodes for lithium-ion batteries. The first step was to prepare GO dispersion *via* a modified Hummers' method. 3 g of graphite powder, 1.5 g of

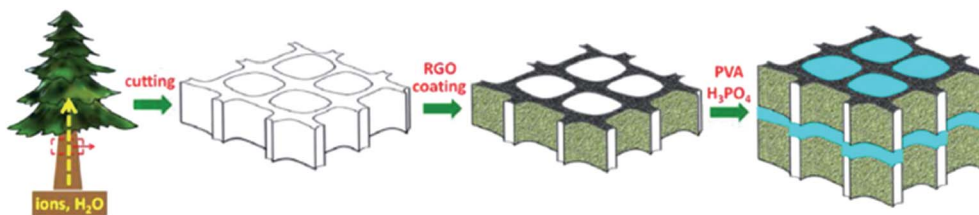


Fig. 15 Illustration of the procedure to fabricate WTSS, WTSS-rGO and the supercapacitor respectively shown. Black and green texture indicates rGO coating, whereas blue texture indicates PVA/H<sub>3</sub>PO<sub>4</sub> gel electrolyte.<sup>179</sup>

NaNO<sub>3</sub> and 69 mL of H<sub>2</sub>SO<sub>4</sub> were mixed together in a beaker, followed by adding 9 g of KMnO<sub>4</sub> and stirred in an ice bath to keep the mixture at 0 °C. The temperature was increased to 35 °C after 30 minutes of stirring. Stirring for an additional 30 minutes, 138 mL of cold deionized water (15 °C) was gradually added. Then, 213 mL of warm water (80 °C) and 15 mL of H<sub>2</sub>O<sub>2</sub> respectively were added. The resulting mixture was placed in a centrifuge to be separated and washed with HCl–H<sub>2</sub>O solution (HCl/H<sub>2</sub>O = 1/10) three times. Finally, the solution was dissolved in deionized water and dispersed homogeneously by ultrasonic agitation for several hours. To synthesize SnO<sub>2</sub>/Graphene aerogels, SnO<sub>2</sub> nanocrystals were prepared by dissolving 2.325 g of SnCl<sub>4</sub>·5H<sub>2</sub>O in 200 mL of deionized water followed by hydrothermal treatment for 160 °C for 16 hours. The resulting precipitate was washed by placing it in a centrifuge three times and re-dispersed in 200 mL of ethanol to produce a suspension. 2.4 mL of SnO<sub>2</sub> dispersion was then added drop-wise into 6 mL of GO (2 mg mL<sup>-1</sup>) (mass ratio 1 : 1). The dispersion was placed in an ultrasonic agitator and stirred for 24 hours to ensure a homogeneous dispersion. Subsequently, 120 mg of ascorbic acid powder was added into the mixture and stirred for 30 minutes. The aforementioned mixture was placed into a mold and into a draught drying cabinet at 75 °C for 4 hours to obtain 3D graphene hydrogels. Then, the monolith was taken out of the mold and immersed in deionized water for 24 hours and freeze-dried into graphene aerogel. Finally, the aerogels were heated to 550 °C for 30 minutes to increase the degree of reduction. The preparation of graphene aerogel as electrodes was the final process. The graphene aerogels were heated at 650 °C for 30 minutes with a N<sub>2</sub> atmosphere. After the heating process, the 3D graphene sheets were used as electrodes without any post-processing.

Another source utilized eco-friendly methods to produce a flexible supercapacitor from wood transverse section slice (WTSS) and reduced graphene oxide.<sup>179</sup> The thickness of a native WTSS was cut from Chinese fir to about 180 μm with rotary microtomy, followed by vacuum drying at 50 °C for 2 hours. Without further purification, graphite powder and 85% aqueous solution of hydrazine hydrate were used to create an aqueous dispersion of graphene oxide (GO) nanosheets with Hummers' method. WTSSs of different areal densities (0.36 mg cm<sup>-2</sup>, 0.49 mg cm<sup>-2</sup>, and 0.68 mg cm<sup>-2</sup>) was immersed in aqueous GO dispersions of 1 mg mL<sup>-1</sup> for 5 min and allowed to dry naturally in room temperature to obtain different GO loadings. The WTSS-GO sheets were then reduced with aqueous

solution of hydrazine hydrate at 90 °C for 3 hours. The finalized results were then rinsed with deionized water and dried in a vacuum at 50 °C for 2 hours. The formation of the supercapacitor was created as seen in Fig. 15. The assembly was seen to utilize the traditional laminated two-electrode configuration with PVA/H<sub>3</sub>PO<sub>4</sub> gel (blue) used as the electrolyte and a separator.

This example describes how researchers devised a way to synthesize a transparent graphene oxide flexible electrode by mixing GO with the conductive polymer in an aqueous solution.<sup>180</sup> First, GO:H<sub>2</sub>O dispersion (15 μg L<sup>-1</sup>) was obtained using the chemical route and the conductive polymer from Sigma-Aldrich [3,4-ethylenedioxythiophene]:poly[styrenesulfonate] (PEDOT:PSS) was purchased. Then 3 mL of GO dispersion was mixed with the desired amount of PEDOT:PSS solution volumes *via* magnetic stirring for 24 hours. The GO dispersion to GO:PEDOT ratio were known to be GO:PEDOT (0.1%), (0.5%), (1.0%), (5.0%), (10.0%) and (20%). Next, polyethylene terephthalate (PET) was used as substrates. GO:PEDOT films were obtained *via* the drop casting method over PET substrates and left to dry at room temperature for 4 hours. After that, it was placed on a hot plate to thermally anneal it at 80 °C at standard room pressure and temperature. Not only are there sustainable ways to fabricate graphene, but also there are environmentally friendly ways to utilize graphene. Like previously mentioned in Hummers' method and exfoliation experiments, along with epitaxial growth and the ability to fabricate it *via* CVD using ethanol as a carbon source on Ni foams, capacitive deionization (CDI) is an effective way to treat wastewater and benefit the environment.<sup>181,182</sup> Heavy metal wastewater pollution has become a problem affecting our environment and water purity as metallurgical and other manufacturing plants increase. Utilizing graphene as an electrode with capacitive deionization to separate and recover heavy metal ions and salt ions in wastewater allows for greater treatment and higher electromagnetic interference shielding effectiveness.<sup>183,184</sup> Current strategies in desalination of saline water include ultrafiltration, reverse osmosis, and distillation processes, but with graphene electrode CDI, it would become the most optimum option.<sup>181,185</sup>

## 4 Summary table

Table 4

Table 4 A summarized synthesis experimental methods

General synthesis method	Experiment	References
Modified Hummers' method	A flexible polyaniline/graphene/bacterial cellulose supercapacitor electrode	186
	Producing large-area, foldable graphene paper from graphite oxide suspensions by an <i>in situ</i> chemical reduction process	187
	Silver fiber fabric as the current collector for preparation of graphene-based supercapacitors	188
	Cu particles induced distinct enhancements for reduced graphene oxide-based flexible supercapacitors	189
	Controllable morphology of polypyrrole wrapped graphene hydrogel framework composites <i>via</i> cyclic voltammetry with aiding of poly(sodium-4-styrene sulfonate) for the flexible supercapacitor electrode	190
	Assembly of graphene aerogels into the 3D biomass-derived carbon frameworks on conductive substrates for flexible supercapacitors	23
Chemical vapor deposition	Superflexible, high-efficiency perovskite solar cells utilizing graphene electrodes: towards future foldable power sources	4
	Graphene-based flexible and stretchable electronics	89
	A graphene foam electrode with sulfur loading for flexible and high energy Li-S batteries	90
	Flexible, sandwich-like CNTs/NiCo <sub>2</sub> O <sub>4</sub> hybrid paper electrodes for all-solid state supercapacitors	95
	Graphene-patched CNT/MnO <sub>2</sub> nanocomposite papers for the electrode of high-performance flexible asymmetric supercapacitors	101
	Reduced graphene oxide-carbon nanotube graphene...	106
Exfoliation of graphite oxide	Continuous mechanical exfoliation of graphene sheets <i>via</i> a three-roll milling system	84
	Preparation of graphitic oxide	16
	An improved Hummers' method for eco-friendly synthesis of graphene oxide	15
	Controllable fabrication of 2D and 3D porous graphene architectures using identical thermally exfoliated graphene oxides as precursors and their application as supercapacitor electrodes	85

## 5 Conclusions

In conclusion, it is evident that the need for furthering graphene's capabilities for application is strong and that there are many approaches one can take to fabricate graphene as a flexible electrode. The incredible interest in graphene can be linked to its ballistic transport at room temperature combined with chemical and mechanical stability.<sup>191</sup> The advancement of portable, wearable, and implantable sensing devices with electrodes can shape the future. Powerful, biocompatible devices at a nanoscale can surely benefit many areas in biomedical engineering.<sup>120,192–200</sup> With the motivation to supply compressed informational and experimental articles, many main and minor fabrication methods were compiled and gone into detail. This was done so that they could be learned from and manipulatable for researchers to fabricate ideal graphene as flexible electrodes. A modified Hummers' method, chemical vapor deposition, and exfoliation of graphite oxide proved as critical methods to use to obtain the desired electrode. Along with that, the quality enhancement techniques support the fabrication methods to create better results. The final portion addresses fabrication methods that prove to be environmentally friendly. As the world takes steps forward in the path toward sustainability, using materials and resources that will not put future generations at risk should always be a priority.<sup>201,202</sup> For this purpose, different methods were addressed to give opportunity to pursue a "green" fabrication process. This review paper does not contain every possible method and factor to fabricate graphene as a flexible electrode, but solemnly addresses common methods used by

researchers. Each method is organized and compiled into multiple tables for quick and easy understanding of advantages and disadvantages as well as fabrication potential.

## Acknowledgements

This work was partially supported by the Office of Naval Research (ONR) Grant N000141612246, ONR Grant N000141712620, and Iowa State University. The authors are grateful for critiques of this manuscript by Jocelyn Chay.

## References

- 1 M. Zhang, C. Hou, A. Halder, H. Wang and Q. Chi, Graphene papers: smart architecture and specific functionalization for biomimetics, electrocatalytic sensing and energy storage, *Mater. Chem. Front.*, 2017, **1**(1), 37–60.
- 2 Y. Xie, P. Yuan, T. Wang, N. Hashemi and X. Wang, Switch on the high thermal conductivity of graphene paper, *Nanoscale*, 2016, **8**(40), 17581–17597.
- 3 Y. Xie, Z. Xu, S. Xu, Z. Cheng, N. Hashemi, C. Deng and X. Wang, The defect level and ideal thermal conductivity of graphene uncovered by residual thermal reffusivity at the 0 K limit, *Nanoscale*, 2015, **7**(22), 10101–10110.
- 4 J. Yoon, H. Sung, G. Lee, W. Cho, N. Ahn, H. S. Jung and M. Choi, Superflexible, high-efficiency perovskite solar cells utilizing graphene electrodes: towards future foldable power sources, *Energy Environ. Sci.*, 2017, **10**, 337–345.

- 5 N. Gao and X. Fang, Synthesis and development of graphene-inorganic semiconductor nanocomposites, *Chem. Rev.*, 2015, **115**(16), 8294–8343.
- 6 P. Liu, T. Yan, L. Shi, H. S. Park, X. Chen, Z. Zhao and D. Zhang, Graphene-based materials for capacitive deionization, *J. Mater. Chem. A*, 2017, **5**(27), 13907–13943.
- 7 Z. Liu, Z. Zhao, Y. Wang, S. Dou, D. Yan, D. Liu, Z. Xia and S. Wang, In Situ Exfoliated, Edge-Rich, Oxygen-Functionalized Graphene from Carbon Fibers for Oxygen Electrocatalysis, *Adv. Mater.*, 2017, **29**, 1606207.
- 8 W. He, Y. Sun, J. Xi, A. A. M. Abdurhman, J. Ren and H. Duan, Printing graphene-carbon nanotube-ionic liquid gel on graphene paper: towards flexible electrodes with efficient loading of PtAu alloy nanoparticles for electrochemical sensing of blood glucose, *Anal. Chim. Acta*, 2016, **903**, 61–68.
- 9 J. S. Friedman, A. Girdhar, R. M. Gelfand, G. Memik, H. Mohseni, A. Tafflove, B. W. Wessels, J.-P. Leburton and A. V. Sahakian, Cascaded spintronic logic with low-dimensional carbon, *Nat. Commun.*, 2017, **8**, 15635.
- 10 A. Rabti, C. C. Mayorga-Martinez, L. Baptista-Pires, N. Raouafi and A. Merkoçi, Ferrocene-functionalized graphene electrode for biosensing applications, *Anal. Chim. Acta*, 2016, **926**, 28–35.
- 11 Y. Aceta and M. Del Valle, Graphene electrode platform for impedimetric aptasensing, *Electrochim. Acta*, 2017, **229**, 458–466.
- 12 T. Kuila, A. K. Mishra, P. Khanra, N. H. Kim and J. H. Lee, Recent advances in the efficient reduction of graphene oxide and its application as energy storage electrode materials, *Nanoscale*, 2013, **5**(1), 52–71.
- 13 D. Zhang, X. Wen, L. Shi, T. Yan and J. Zhang, Enhanced capacitive deionization of graphene/mesoporous carbon composites, *Nanoscale*, 2012, **4**(17), 5440–5446.
- 14 H. Yu, B. Zhang, C. Bulin, R. Li and R. Xing, High-efficient Synthesis of Graphene Oxide Based on Improved Hummers Method, *Sci. Rep.*, 2016, **6**, 36143.
- 15 J. Chen, B. Yao, C. Li and G. Shi, An improved Hummers method for eco-friendly synthesis of graphene oxide, *Carbon*, 2013, **64**, 225–229.
- 16 W. S. Hummers Jr and R. E. Offeman, Preparation of graphitic oxide, *J. Am. Chem. Soc.*, 1958, **80**(6), 1339.
- 17 D. Konios, C. Petridis, G. Kakavelakis, M. Sygletou, K. Savva, E. Stratakis and E. Kymakis, Reduced graphene oxide micromesh electrodes for large area, flexible, organic photovoltaic devices, *Adv. Funct. Mater.*, 2015, **25**(15), 2213–2221.
- 18 J.-D. Qiu, G.-C. Wang, R.-P. Liang, X.-H. Xia and H.-W. Yu, Controllable deposition of platinum nanoparticles on graphene as an electrocatalyst for direct methanol fuel cells, *J. Phys. Chem. C*, 2011, **115**(31), 15639–15645.
- 19 X. Lu, H. Dou, S. Yang, L. Hao, L. Zhang, L. Shen, F. Zhang and X. Zhang, Fabrication and electrochemical capacitance of hierarchical graphene/polyaniline/carbon nanotube ternary composite film, *Electrochim. Acta*, 2011, **56**(25), 9224–9232.
- 20 A. Zhao, Z. Zhang, P. Zhang, S. Xiao, L. Wang, Y. Dong, H. Yuan, P. Li, Y. Sun and X. Jiang, 3D nanoporous gold scaffold supported on graphene paper: Freestanding and flexible electrode with high loading of ultrafine PtCo alloy nanoparticles for electrochemical glucose sensing, *Anal. Chim. Acta*, 2016, **938**, 63–71.
- 21 F. Xiao, S. Yang, Z. Zhang, H. Liu, J. Xiao, L. Wan, J. Luo, S. Wang and Y. Liu, Scalable synthesis of freestanding sandwich-structured graphene/polyaniline/graphene nanocomposite paper for flexible all-solid-state supercapacitor, *Sci. Rep.*, 2015, **5**, 9359.
- 22 F. Xiao, Y. Li, X. Zan, K. Liao, R. Xu and H. Duan, Growth of metal-metal oxide nanostructures on freestanding graphene paper for flexible biosensors, *Adv. Funct. Mater.*, 2012, **22**(12), 2487–2494.
- 23 Y.-M. Fan, W.-L. Song, X. Li and L.-Z. Fan, Assembly of graphene aerogels into the 3D biomass-derived carbon frameworks on conductive substrates for flexible supercapacitors, *Carbon*, 2017, **111**, 658–666.
- 24 F. Bonaccorso, L. Colombo, G. Yu, M. Stoller, V. Tozzini, A. C. Ferrari, R. S. Ruoff and V. Pellegrini, Graphene, related two-dimensional crystals, and hybrid systems for energy conversion and storage, *Science*, 2015, **347**(6217), 1246501.
- 25 S. Han, D. Wu, S. Li, F. Zhang and X. Feng, Porous graphene materials for advanced electrochemical energy storage and conversion devices, *Adv. Mater.*, 2014, **26**(6), 849–864.
- 26 C. Wan, Y. Jiao and J. Li, Flexible, highly conductive, and free-standing reduced graphene oxide/polypyrrole/cellulose hybrid papers for supercapacitor electrodes, *J. Mater. Chem. A*, 2017, **5**, 3819–3831.
- 27 Z. Weng, Y. Su, D. W. Wang, F. Li, J. Du and H. M. Cheng, Graphene-cellulose paper flexible supercapacitors, *Adv. Energy Mater.*, 2011, **1**(5), 917–922.
- 28 L. Yuan, B. Yao, B. Hu, K. Huo, W. Chen and J. Zhou, Polypyrrole-coated paper for flexible solid-state energy storage, *Energy Environ. Sci.*, 2013, **6**(2), 470–476.
- 29 V. L. Pushparaj, M. M. Shaijumon, A. Kumar, S. Murugesan, L. Ci, R. Vajtai, R. J. Linhardt, O. Nalamasu and P. M. Ajayan, Flexible energy storage devices based on nanocomposite paper, *Proc. Natl. Acad. Sci. U. S. A.*, 2007, **104**(34), 13574–13577.
- 30 L. Liu, Z. Niu, L. Zhang, W. Zhou, X. Chen and S. Xie, Nanostructured graphene composite papers for highly flexible and foldable supercapacitors, *Adv. Mater.*, 2014, **26**(28), 4855–4862.
- 31 S. D. Perera, B. Patel, N. Nijem, K. Roodenko, O. Seitz, J. P. Ferraris, Y. J. Chabal and K. J. Balkus, Vanadium Oxide Nanowire-Carbon Nanotube Binder-Free Flexible Electrodes for Supercapacitors, *Adv. Energy Mater.*, 2011, **1**(5), 936–945.
- 32 M. Mastragostino, C. Arbizzani, L. Meneghello and R. Paraventi, Electronically conducting polymers and activated carbon: electrode materials in supercapacitor technology, *Adv. Mater.*, 1996, **8**(4), 331–334.

- 33 G. A. Snook, P. Kao and A. S. Best, Conducting-polymer-based supercapacitor devices and electrodes, *J. Power Sources*, 2011, **196**(1), 1–12.
- 34 F. Sharifi, S. Ghobadian, F. R. Cavalcanti and N. Hashemi, Paper-based devices for energy applications, *Renewable Sustainable Energy Rev.*, 2015, **52**, 1453–1472.
- 35 N. Hashemi, J. M. Lackore, F. Sharifi, P. J. Goodrich, M. L. Winchell and N. Hashemi, A paper-based microbial fuel cell operating under continuous flow condition, *Technology*, 2016, **04**(02), 98–103.
- 36 D. Sechi, B. Greer, J. Johnson and N. Hashemi, Three-Dimensional Paper-Based Microfluidic Device for Assays of Protein and Glucose in Urine, *Anal. Chem.*, 2013, **85**(22), 10733–10737.
- 37 L. T. Wagner, N. Hashemi and N. Hashemi, *A Compact Versatile Microbial Fuel Cell From Paper*, 2013, p. V001T01A15, 55522.
- 38 L. Wen, K. Li, J. Liu, Y. Huang, F. Bu, B. Zhao and Y. Xu, Graphene/polyaniline@ carbon cloth composite as a high-performance flexible supercapacitor electrode prepared by a one-step electrochemical co-deposition method, *RSC Adv.*, 2017, **7**(13), 7688–7693.
- 39 Y. Meng, K. Wang, Y. Zhang and Z. Wei, Hierarchical porous graphene/polyaniline composite film with superior rate performance for flexible supercapacitors, *Adv. Mater.*, 2013, **25**(48), 6985–6990.
- 40 C. Liu, F. Li, L. P. Ma and H. M. Cheng, Advanced materials for energy storage, *Adv. Mater.*, 2010, **22**, E28–E62.
- 41 Y. Yan, Y. Zhang, W. Hu and Z. Wei, Hierarchical crystalline superstructures of conducting polymers with homohelicity, *Chem.–Eur. J.*, 2010, **16**(29), 8626–8630.
- 42 F. Liu, S. Song, D. Xue and H. Zhang, Folded structured graphene paper for high performance electrode materials, *Adv. Mater.*, 2012, **24**(8), 1089–1094.
- 43 Y. Zhu, S. Murali, W. Cai, X. Li, J. W. Suk, J. R. Potts and R. S. Ruoff, Graphene and graphene oxide: synthesis, properties, and applications, *Adv. Mater.*, 2010, **22**(35), 3906–3924.
- 44 M. D. Stoller, S. Park, Y. Zhu, J. An and R. S. Ruoff, Graphene-based ultracapacitors, *Nano Lett.*, 2008, **8**(10), 3498–3502.
- 45 D. Tobjörk and R. Österbacka, Paper Electronics, *Adv. Mater.*, 2011, **23**(17), 1935–1961.
- 46 Y. G. Wang, H. Q. Li and Y. Y. Xia, Ordered Whiskerlike Polyaniline Grown on the Surface of Mesoporous Carbon and Its Electrochemical Capacitance Performance, *Adv. Mater.*, 2006, **18**(19), 2619–2623.
- 47 Y.-E. Miao, W. Fan, D. Chen and T. Liu, High-performance supercapacitors based on hollow polyaniline nanofibers by electrospinning, *ACS Appl. Mater. Interfaces*, 2013, **5**(10), 4423–4428.
- 48 S. Wang, N. Liu, J. Su, L. Li, F. Long, Z. Zou, X. Jiang and Y. Gao, Highly Stretchable and Self-Healable Supercapacitor with Reduced Graphene Oxide Based Fiber Springs, *ACS Nano*, 2017, **11**(2), 2066–2074.
- 49 Y. Kim, J. Zhu, B. Yeom, M. Di Prima, X. Su, J.-G. Kim, S. J. Yoo, C. Uher and N. A. Kotov, Stretchable nanoparticle conductors with self-organized conductive pathways, *Nature*, 2013, **500**(7460), 59–63.
- 50 B. Y. Ahn, E. B. Duoss, M. J. Motala, X. Guo, S.-I. Park, Y. Xiong, J. Yoon, R. G. Nuzzo, J. A. Rogers and J. A. Lewis, Omnidirectional Printing of Flexible, Stretchable, and Spanning Silver Microelectrodes, *Science*, 2009, **323**(5921), 1590–1593.
- 51 Y. Wang, R. Yang, Z. Shi, L. Zhang, D. Shi, E. Wang and G. Zhang, Super-Elastic Graphene Ripples for Flexible Strain Sensors, *ACS Nano*, 2011, **5**(5), 3645–3650.
- 52 Y. Huang, M. Zhong, Y. Huang, M. Zhu, Z. Pei, Z. Wang, Q. Xue, X. Xie and C. Zhi, A self-healable and highly stretchable supercapacitor based on a dual crosslinked polyelectrolyte, *Nat. Commun.*, 2015, **6**, 10310.
- 53 Y. Xu, Y. Zhang, Z. Guo, J. Ren, Y. Wang and H. Peng, Flexible, Stretchable, and Rechargeable Fiber-Shaped Zinc–Air Battery Based on Cross-Stacked Carbon Nanotube Sheets, *Angew. Chem., Int. Ed.*, 2015, **54**(51), 15390–15394.
- 54 Y. Xie, Y. Liu, Y. Zhao, Y. H. Tsang, S. P. Lau, H. Huang and Y. Chai, Stretchable all-solid-state supercapacitor with wavy shaped polyaniline/graphene electrode, *J. Mater. Chem. A*, 2014, **2**(24), 9142–9149.
- 55 X. Li, T. Gu and B. Wei, Dynamic and Galvanic Stability of Stretchable Supercapacitors, *Nano Lett.*, 2012, **12**(12), 6366–6371.
- 56 J. Tao, N. Liu, W. Ma, L. Ding, L. Li, J. Su and Y. Gao, Solid-State High Performance Flexible Supercapacitors Based on Polypyrrole-MnO<sub>2</sub>-Carbon Fiber Hybrid Structure, *Sci. Rep.*, 2013, **3**, 2286.
- 57 N. Liu, W. Ma, J. Tao, X. Zhang, J. Su, L. Li, C. Yang, Y. Gao, D. Golberg and Y. Bando, Cable-Type Supercapacitors of Three-Dimensional Cotton Thread Based Multi-Grade Nanostructures for Wearable Energy Storage, *Adv. Mater.*, 2013, **25**(35), 4925–4931.
- 58 H. Sun, X. You, J. Deng, X. Chen, Z. Yang, J. Ren and H. Peng, Novel Graphene/Carbon Nanotube Composite Fibers for Efficient Wire-Shaped Miniature Energy Devices, *Adv. Mater.*, 2014, **26**(18), 2868–2873.
- 59 K. S. Novoselov, A. K. Geim, S. V. Morozov, D. Jiang, M. I. Katsnelson, I. V. Grigorieva, S. V. Dubonos and A. A. Firsov, Two-dimensional gas of massless Dirac fermions in graphene, *Nature*, 2005, **438**(7065), 197–200.
- 60 C. Lee, X. Wei, J. W. Kysar and J. Hone, Measurement of the Elastic Properties and Intrinsic Strength of Monolayer Graphene, *Science*, 2008, **321**(5887), 385–388.
- 61 Z. Yang, H. Sun, T. Chen, L. Qiu, Y. Luo and H. Peng, Photovoltaic Wire Derived from a Graphene Composite Fiber Achieving an 8.45 % Energy Conversion Efficiency, *Angew. Chem.*, 2013, **125**(29), 7693–7696.
- 62 Z. Dong, C. Jiang, H. Cheng, Y. Zhao, G. Shi, L. Jiang and L. Qu, Facile Fabrication of Light, Flexible and Multifunctional Graphene Fibers, *Adv. Mater.*, 2012, **24**(14), 1856–1861.
- 63 L. Huang, N. Yi, Y. Wu, Y. Zhang, Q. Zhang, Y. Huang, Y. Ma and Y. Chen, Multichannel and Repeatable Self-Healing of Mechanical Enhanced Graphene-Thermoplastic

- Polyurethane Composites, *Adv. Mater.*, 2013, **25**(15), 2224–2228.
- 64 C. Wang, N. Liu, R. Allen, J. B. H. Tok, Y. Wu, F. Zhang, Y. Chen and Z. A. Bao, Rapid and Efficient Self-Healing Thermo-Reversible Elastomer Crosslinked with Graphene Oxide, *Adv. Mater.*, 2013, **25**(40), 5785–5790.
- 65 M. D. Hager, P. Greil, C. Leyens, S. van der Zwaag and U. S. Schubert, Self-Healing Materials, *Adv. Mater.*, 2010, **22**(47), 5424–5430.
- 66 Y. Huang, M. Zhu, Y. Huang, Z. Pei, H. Li, Z. Wang, Q. Xue and C. Zhi, Multifunctional Energy Storage and Conversion Devices, *Adv. Mater.*, 2016, **28**(38), 8344–8364.
- 67 H. Wang, B. Zhu, W. Jiang, Y. Yang, W. R. Leow, H. Wang and X. Chen, Supercapacitors: A Mechanically and Electrically Self-Healing Supercapacitor (Adv. Mater. 22/2014), *Adv. Mater.*, 2014, **26**(22), 3637.
- 68 Y. Huang, Y. Huang, M. Zhu, W. Meng, Z. Pei, C. Liu, H. Hu and C. Zhi, Magnetic-Assisted, Self-Healable, Yarn-Based Supercapacitor, *ACS Nano*, 2015, **9**(6), 6242–6251.
- 69 W. Liu, N. Liu, Y. Shi, Y. Chen, C. Yang, J. Tao, S. Wang, Y. Wang, J. Su, L. Li and Y. Gao, A wire-shaped flexible asymmetric supercapacitor based on carbon fiber coated with a metal oxide and a polymer, *J. Mater. Chem. A*, 2015, **3**(25), 13461–13467.
- 70 X. Wang, S.-X. Zhao, L. Dong, Q.-L. Lu, J. Zhu and C.-W. Nan, One-step synthesis of surface-enriched nickel cobalt sulfide nanoparticles on graphene for high-performance supercapacitors, *Energy Storage Materials*, 2017, **6**, 180–187.
- 71 H. Chen, J. Jiang, L. Zhang, H. Wan, T. Qi and D. Xia, Highly conductive NiCo<sub>2</sub>S<sub>4</sub> urchin-like nanostructures for high-rate pseudocapacitors, *Nanoscale*, 2013, **5**(19), 8879–8883.
- 72 X. Xiong, G. Waller, D. Ding, D. Chen, B. Rainwater, B. Zhao, Z. Wang and M. Liu, Controlled synthesis of NiCo<sub>2</sub>S<sub>4</sub> nanostructured arrays on carbon fiber paper for high-performance pseudocapacitors, *Nano Energy*, 2015, **16**, 71–80.
- 73 H. Chen, L. Hu, M. Chen, Y. Yan and L. Wu, Nickel-Cobalt Layered Double Hydroxide Nanosheets for High-performance Supercapacitor Electrode Materials, *Adv. Funct. Mater.*, 2014, **24**(7), 934–942.
- 74 J. Pu, T. Wang, H. Wang, Y. Tong, C. Lu, W. Kong and Z. Wang, Direct Growth of NiCo<sub>2</sub>S<sub>4</sub> Nanotube Arrays on Nickel Foam as High-Performance Binder-Free Electrodes for Supercapacitors, *ChemPlusChem*, 2014, **79**(4), 577–583.
- 75 X. Meng, J. Deng, J. Zhu, H. Bi, E. Kan and X. Wang, Cobalt Sulfide/Graphene Composite Hydrogel as Electrode for High-Performance Pseudocapacitors, *Sci. Rep.*, 2016, **6**, 21717.
- 76 R. Wu, D. P. Wang, X. Rui, B. Liu, K. Zhou, A. W. K. Law, Q. Yan, J. Wei and Z. Chen, In-Situ Formation of Hollow Hybrids Composed of Cobalt Sulfides Embedded within Porous Carbon Polyhedra/Carbon Nanotubes for High-Performance Lithium-Ion Batteries, *Adv. Mater.*, 2015, **27**(19), 3038–3044.
- 77 W. Chen, C. Xia and H. N. Alshareef, One-Step Electrodeposited Nickel Cobalt Sulfide Nanosheet Arrays for High-Performance Asymmetric Supercapacitors, *ACS Nano*, 2014, **8**(9), 9531–9541.
- 78 P. Wen, M. Fan, D. Yang, Y. Wang, H. Cheng and J. Wang, An asymmetric supercapacitor with ultrahigh energy density based on nickel cobalt sulfide nanocluster anchoring multi-wall carbon nanotubes hybrid, *J. Power Sources*, 2016, **320**, 28–36.
- 79 H. Wang, D. Zhang, T. Yan, X. Wen, J. Zhang, L. Shi and Q. Zhong, Three-dimensional macroporous graphene architectures as high performance electrodes for capacitive deionization, *J. Mater. Chem. A*, 2013, **1**(38), 11778–11789.
- 80 P. Liu, H. Wang, T. Yan, J. Zhang, L. Shi and D. Zhang, Grafting sulfonic and amine functional groups on 3D graphene for improved capacitive deionization, *J. Mater. Chem. A*, 2016, **4**(14), 5303–5313.
- 81 X. Wen, D. Zhang, T. Yan, J. Zhang and L. Shi, Three-dimensional graphene-based hierarchically porous carbon composites prepared by a dual-template strategy for capacitive deionization, *J. Mater. Chem. A*, 2013, **1**(39), 12334–12344.
- 82 J. Zhang, Y. Jin, C. Li, Y. Shen, L. Han, Z. Hu, X. Di and Z. Liu, Creation of three-dimensionally ordered macroporous Au/CeO<sub>2</sub> catalysts with controlled pore sizes and their enhanced catalytic performance for formaldehyde oxidation, *Appl. Catal., B*, 2009, **91**(1), 11–20.
- 83 H. Wang, L. Shi, T. Yan, J. Zhang, Q. Zhong and D. Zhang, Design of graphene-coated hollow mesoporous carbon spheres as high performance electrodes for capacitive deionization, *J. Mater. Chem. A*, 2014, **2**(13), 4739–4750.
- 84 J. Chen, M. Duan and G. Chen, Continuous mechanical exfoliation of graphene sheets via three-roll mill, *J. Mater. Chem.*, 2012, **22**(37), 19625–19628.
- 85 K. Xia, Q. Li, L. Zheng, K. You, X. Tian, B. Han, Q. Gao, Z. Huang, G. Chen and C. Zhou, Controllable fabrication of 2D and 3D porous graphene architectures using identical thermally exfoliated graphene oxides as precursors and their application as supercapacitor electrodes, *Microporous Mesoporous Mater.*, 2017, **237**, 228–236.
- 86 Y. Zou and S. Wang, Interconnecting Carbon Fibers with the In-situ Electrochemically Exfoliated Graphene as Advanced Binder-free Electrode Materials for Flexible Supercapacitor, *Sci. Rep.*, 2015, **5**, 11792.
- 87 H. Tetlow, J. P. de Boer, I. Ford, D. Vvedensky, J. Coraux and L. Kantorovich, Growth of epitaxial graphene: theory and experiment, *Phys. Rep.*, 2014, **542**(3), 195–295.
- 88 Y. He, W. Chen, X. Li, Z. Zhang, J. Fu, C. Zhao and E. Xie, Freestanding three-dimensional graphene/MnO<sub>2</sub> composite networks as ultralight and flexible supercapacitor electrodes, *ACS Nano*, 2012, **7**(1), 174–182.
- 89 H. Jang, Y. J. Park, X. Chen, T. Das, M. S. Kim and J. H. Ahn, Graphene-Based Flexible and Stretchable Electronics, *Adv. Mater.*, 2016, **28**, 4184–4202.
- 90 G. Zhou, L. Li, C. Ma, S. Wang, Y. Shi, N. Koratkar, W. Ren, F. Li and H.-M. Cheng, A graphene foam electrode with

- high sulfur loading for flexible and high energy Li-S batteries, *Nano Energy*, 2015, **11**, 356–365.
- 91 A. Manthiram, Y. Fu and Y.-S. Su, Challenges and prospects of lithium–sulfur batteries, *Acc. Chem. Res.*, 2012, **46**(5), 1125–1134.
- 92 S. S. Zhang and D. T. Tran, A proof-of-concept lithium/sulfur liquid battery with exceptionally high capacity density, *J. Power Sources*, 2012, **211**, 169–172.
- 93 Z. Chen, W. Ren, L. Gao, B. Liu, S. Pei and H.-M. Cheng, Three-dimensional flexible and conductive interconnected graphene networks grown by chemical vapour deposition, *Nat. Mater.*, 2011, **10**(6), 424–428.
- 94 Z. Chen, C. Xu, C. Ma, W. Ren and H. M. Cheng, Lightweight and flexible graphene foam composites for high-performance electromagnetic interference shielding, *Adv. Mater.*, 2013, **25**(9), 1296–1300.
- 95 Y. Zheng, Z. Lin, W. Chen, B. Liang, H. Du, R. Yang, X. He, Z. Tang and X. Gui, Flexible, sandwich-like CNTs/NiCo<sub>2</sub>O<sub>4</sub> hybrid paper electrodes for all-solid state supercapacitors, *J. Mater. Chem. A*, 2017, **5**(12), 5886–5894.
- 96 F. Cai, Y. Kang, H. Chen, M. Chen and Q. Li, Hierarchical CNT@ NiCo<sub>2</sub>O<sub>4</sub> core-shell hybrid nanostructure for high-performance supercapacitors, *J. Mater. Chem. A*, 2014, **2**(29), 11509–11515.
- 97 T. Y. Wei, C. H. Chen, H. C. Chien, S. Y. Lu and C. C. Hu, A cost-effective supercapacitor material of ultrahigh specific capacitances: spinel nickel cobaltite aerogels from an epoxide-driven sol-gel process, *Adv. Mater.*, 2010, **22**(3), 347–351.
- 98 G. Zhang and X. W. D. Lou, General Solution Growth of Mesoporous NiCo<sub>2</sub>O<sub>4</sub> Nanosheets on Various Conductive Substrates as High-Performance Electrodes for Supercapacitors, *Adv. Mater.*, 2013, **25**(7), 976–979.
- 99 D. Kong, W. Ren, C. Cheng, Y. Wang, Z. Huang and H. Y. Yang, Three-dimensional NiCo<sub>2</sub>O<sub>4</sub>@ polypyrrole coaxial nanowire arrays on carbon textiles for high-performance flexible asymmetric solid-state supercapacitor, *ACS Appl. Mater. Interfaces*, 2015, **7**(38), 21334–21346.
- 100 X. Zhao, B. M. Sánchez, P. J. Dobson and P. S. Grant, The role of nanomaterials in redox-based supercapacitors for next generation energy storage devices, *Nanoscale*, 2011, **3**(3), 839–855.
- 101 Y. Jin, H. Chen, M. Chen, N. Liu and Q. Li, Graphene-patched CNT/MnO<sub>2</sub> nanocomposite papers for the electrode of high-performance flexible asymmetric supercapacitors, *ACS Appl. Mater. Interfaces*, 2013, **5**(8), 3408–3416.
- 102 M. Lu, F. Sharifi, N. N. Hashemi and R. Montazami, Fluid-Induced Alignment of Carbon Nanofibers in Polymer Fibers, *Macromol. Mater. Eng.*, 2017, **302**, 1600544.
- 103 P. Simon and Y. Gogotsi, Materials for electrochemical capacitors, *Nat. Mater.*, 2008, **7**(11), 845–854.
- 104 M. R. Bailey and S. W. Donne, The effect of barium hydroxide on the rechargeable performance of alkaline  $\gamma$ -MnO<sub>2</sub>, *J. Electrochem. Soc.*, 2012, **159**(7), A999–A1004.
- 105 D. Li, M. B. Müller, S. Gilje, R. B. Kaner and G. G. Wallace, Processable aqueous dispersions of graphene nanosheets, *Nat. Nanotechnol.*, 2008, **3**(2), 101–105.
- 106 C. Xiong, T. Li, T. Zhao, A. Dang, H. Li, X. Ji, W. Jin, S. Jiao, Y. Shang and Y. Zhang, Reduced graphene oxide-carbon nanotube grown on carbon fiber as binder-free electrode for flexible high-performance fiber supercapacitors, *Composites, Part B*, 2017, **116**, 7–15.
- 107 M. R. Atiyah, D. A. Biak, F. Ahmadun, I. Ahamad, F. M. Yasin and H. M. Yusoff, Low temperature growth of vertically aligned carbon nanotubes *via* floating catalyst chemical vapor deposition method, *J. Mater. Sci. Technol.*, 2011, **27**(4), 296–300.
- 108 G. Formica and W. Lacarbonara, A nonlinear mechanical model for the fatigue life of thin-film carbon nanotube supercapacitors, *Composites, Part B*, 2015, **80**, 299–306.
- 109 A. Ghosh and Y. H. Lee, Carbon-Based Electrochemical Capacitors, *ChemSusChem*, 2012, **5**(3), 480–499.
- 110 L. L. Zhang, R. Zhou and X. S. Zhao, Graphene-based materials as supercapacitor electrodes, *J. Mater. Chem.*, 2010, **20**(29), 5983–5992.
- 111 Y. Zhai, Y. Dou, D. Zhao, P. F. Fulvio, R. T. Mayes and S. Dai, Carbon Materials for Chemical Capacitive Energy Storage, *Adv. Mater.*, 2011, **23**(42), 4828–4850.
- 112 Y. Shang, T. Li, H. Li, A. Dang, L. Zhang, Y. Yin, C. Xiong and T. Zhao, Preparation and characterization of graphene derived from low-temperature and pressure promoted thermal reduction, *Composites, Part B*, 2016, **99**, 106–111.
- 113 C. Xiong, T. Li, T. Zhao, Y. Shang, A. Dang, X. Ji, H. Li and J. Wang, Two – step approach of fabrication of three – dimensional reduced graphene oxide – carbon nanotubes – nickel foams hybrid as a binder – free supercapacitor electrode, *Electrochim. Acta*, 2016, **217**, 9–15.
- 114 Z. Yang, R. Gao, N. Hu, J. Chai, Y. Cheng, L. Zhang, H. Wei, E. S.-W. Kong and Y. Zhang, The prospective two-dimensional graphene nanosheets: preparation, functionalization and applications, *Nano-Micro Lett.*, 2012, **4**(1), 1–9.
- 115 P. W. Sutter, J.-I. Flege and E. A. Sutter, Epitaxial graphene on ruthenium, *Nat. Mater.*, 2008, **7**(5), 406–411.
- 116 H.-F. Yen, Y.-Y. Horng, M.-S. Hu, W.-H. Yang, J.-R. Wen, A. Ganguly, Y. Tai, K.-H. Chen and L.-C. Chen, Vertically aligned epitaxial graphene nanowalls with dominated nitrogen doping for superior supercapacitors, *Carbon*, 2015, **82**, 124–134.
- 117 N. K. Mahenderkar, Q. Chen, Y.-C. Liu, A. R. Duchild, S. Hofheins, E. Chason and J. A. Switzer, Epitaxial lift-off of electrodeposited single-crystal gold foils for flexible electronics, *Science*, 2017, **355**(6330), 1203–1206.
- 118 D. Akinwande, N. Petrone and J. Hone, Two-dimensional flexible nanoelectronics, *Nat. Commun.*, 2014, **5**, 5678.
- 119 W. Gao, S. Emaminejad, H. Y. Y. Nyein, S. Challa, K. Chen, A. Peck, H. M. Fahad, H. Ota, H. Shiraki and D. Kiriya, Fully integrated wearable sensor arrays for multiplexed *in situ* perspiration analysis, *Nature*, 2016, **529**(7587), 509–514.



- 120 B. D. Gates, Flexible Electronics, *Science*, 2009, **323**(5921), 1566–1567.
- 121 J. A. Rogers, T. Someya and Y. Huang, Materials and Mechanics for Stretchable Electronics, *Science*, 2010, **327**(5973), 1603–1607.
- 122 J. C. Yeo and C. T. Lim, Emerging flexible and wearable physical sensing platforms for healthcare and biomedical applications, *Microsyst. Nanoeng.*, 2016, **2**, 16043.
- 123 J. B. Vander Wiel, J. D. Mikulicz, M. R. Boysen, N. Hashemi, P. Kalgren, L. Nauman, S. J. Baetzold, G. G. Powell, Q. He and N. N. Hashemi, Characterization of *Chlorella vulgaris* and *Chlorella protothecoides* using multi-pixel photon counters in a 3D focusing optofluidic system, *RSC Adv.*, 2017, **7**(8), 4402–4408.
- 124 J. A. Koza, J. C. Hill, A. C. Demster and J. A. Switzer, Epitaxial electrodeposition of methylammonium lead iodide perovskites, *Chem. Mater.*, 2015, **28**(1), 399–405.
- 125 J. W. Shin, A. Standley and E. Chason, Epitaxial electrodeposition of freestanding large area single crystal substrates, *Appl. Phys. Lett.*, 2007, **90**(26), 261909.
- 126 S. Warren, P. Prod'homme, F. Maroun, P. Allongue, R. Cortès, C. Ferrero, T.-L. Lee, B. Cowie, C. Walker and S. Ferrer, Electrochemical Au deposition on stepped Si (111)-H surfaces: 3D versus 2D growth studied by AFM and X-ray diffraction, *Surf. Sci.*, 2009, **603**(9), 1212–1220.
- 127 P. Prod'Homme, F. Maroun, R. Cortes and P. Allongue, Electrochemical growth of ultraflat Au (111) epitaxial buffer layers on H-Si (111), *Appl. Phys. Lett.*, 2008, **93**(17), 171901.
- 128 J. Chen, Y. Li, L. Huang, C. Li and G. Shi, High-yield preparation of graphene oxide from small graphite flakes via an improved Hummers method with a simple purification process, *Carbon*, 2015, **81**, 826–834.
- 129 Z.-Y. Juang, C.-Y. Wu, A.-Y. Lu, C.-Y. Su, K.-C. Leou, F.-R. Chen and C.-H. Tsai, Graphene synthesis by chemical vapor deposition and transfer by a roll-to-roll process, *Carbon*, 2010, **48**(11), 3169–3174.
- 130 T. Kobayashi, M. Bando, N. Kimura, K. Shimizu, K. Kadono, N. Umezū, K. Miyahara, S. Hayazaki, S. Nagai and Y. Mizuguchi, Production of a 100-m-long high-quality graphene transparent conductive film by roll-to-roll chemical vapor deposition and transfer process, *Appl. Phys. Lett.*, 2013, **102**(2), 023112.
- 131 T. Yamada, M. Ishihara, J. Kim, M. Hasegawa and S. Iijima, A roll-to-roll microwave plasma chemical vapor deposition process for the production of 294 mm width graphene films at low temperature, *Carbon*, 2012, **50**(7), 2615–2619.
- 132 H. Chang, G. Wang, A. Yang, X. Tao, X. Liu, Y. Shen and Z. Zheng, A transparent, flexible, low-temperature, and solution-processible graphene composite electrode, *Adv. Funct. Mater.*, 2010, **20**(17), 2893–2902.
- 133 A. S. Plaut, U. Wurstbauer, S. Wang, A. L. Levy, L. F. dos Santos, L. Wang, L. N. Pfeiffer, K. Watanabe, T. Taniguchi and C. R. Dean, Exceptionally large migration length of carbon and topographically-facilitated self-limiting molecular beam epitaxial growth of graphene on hexagonal boron nitride, *Carbon*, 2017, **114**, 579–584.
- 134 H. Lei, T. Yan, H. Wang, L. Shi, J. Zhang and D. Zhang, Graphene-like carbon nanosheets prepared by a Fe-catalyzed glucose-blowing method for capacitive deionization, *J. Mater. Chem. A*, 2015, **3**(11), 5934–5941.
- 135 D. Yan, S. Dou, L. Tao, Z. Liu, Z. Liu, J. Huo and S. Wang, Electropolymerized supermolecule derived N, P co-doped carbon nanofiber networks as a highly efficient metal-free electrocatalyst for the hydrogen evolution reaction, *J. Mater. Chem. A*, 2016, **4**(36), 13726–13730.
- 136 X. Lu, H. Dou and X. Zhang, Mesoporous carbon nanospheres inserting into graphene sheets for flexible supercapacitor film electrode, *Mater. Lett.*, 2016, **178**, 304–307.
- 137 G. Eda, G. Fanchini and M. Chhowalla, Large-area ultrathin films of reduced graphene oxide as a transparent and flexible electronic material, *Nat. Nanotechnol.*, 2008, **3**(5), 270–274.
- 138 W. K. Chee, H. N. Lim, Z. Zainal, N. M. Huang, I. Harrison and Y. Andou, Flexible graphene-based supercapacitors: a review, *J. Phys. Chem. C*, 2016, **120**(8), 4153–4172.
- 139 S. Bae, H. Kim, Y. Lee, X. Xu, J.-S. Park, Y. Zheng, J. Balakrishnan, T. Lei, H. R. Kim and Y. I. Song, Roll-to-roll production of 30-inch graphene films for transparent electrodes, *Nat. Nanotechnol.*, 2010, **5**(8), 574–578.
- 140 B. Deng, P.-C. Hsu, G. Chen, B. Chandrashekar, L. Liao, Z. Aytimuda, J. Wu, Y. Guo, L. Lin and Y. Zhou, Roll-to-roll encapsulation of metal nanowires between graphene and plastic substrate for high-performance flexible transparent electrodes, *Nano Lett.*, 2015, **15**(6), 4206–4213.
- 141 J. Luque-Garcia and M. L. De Castro, Ultrasound: a powerful tool for leaching, *TrAC, Trends Anal. Chem.*, 2003, **22**(1), 41–47.
- 142 R. S. Edwards and K. S. Coleman, Graphene synthesis: relationship to applications, *Nanoscale*, 2013, **5**(1), 38–51.
- 143 L. Gao, J. U. Surjadi, K. Cao, H. Zhang, P. Li, S. Xu, C. Jiang, J. Song, D. Sun and Y. Lu, Flexible Fiber-Shaped Supercapacitor Based on Nickel–Cobalt Double Hydroxide and Pen Ink Electrodes on Metallized Carbon Fiber, *ACS Appl. Mater. Interfaces*, 2017, **9**(6), 5409–5418.
- 144 Y. Fu, X. Cai, H. Wu, Z. Lv, S. Hou, M. Peng, X. Yu and D. Zou, Fiber supercapacitors utilizing pen ink for flexible/wearable energy storage, *Adv. Mater.*, 2012, **24**(42), 5713–5718.
- 145 L. Liu, Y. Yu, C. Yan, K. Li and Z. Zheng, Wearable energy-dense and power-dense supercapacitor yarns enabled by scalable graphene-metallic textile composite electrodes, *Nat. Commun.*, 2015, **6**, 7260.
- 146 C. Choi, S. H. Kim, H. J. Sim, J. A. Lee, A. Y. Choi, Y. T. Kim, X. Lepró, G. M. Spinks, R. H. Baughman and S. J. Kim, Stretchable, weavable coiled carbon nanotube/MnO<sub>2</sub>/polymer fiber solid-state supercapacitors, *Sci. Rep.*, 2015, **5**, 9387.
- 147 J. Di, X. Zhang, Z. Yong, Y. Zhang, D. Li, R. Li and Q. Li, Carbon-Nanotube Fibers for Wearable Devices and Smart Textiles, *Adv. Mater.*, 2016, **28**(47), 10529–10538.
- 148 W. Cai, T. Lai, J. Lai, H. Xie, L. Ouyang, J. Ye and C. Yu, Transition metal sulfides grown on graphene fibers for

- wearable asymmetric supercapacitors with high volumetric capacitance and high energy density, *Sci. Rep.*, 2016, **6**, 26890.
- 149 J. Sun, Y. Huang, C. Fu, Z. Wang, Y. Huang, M. Zhu, C. Zhi and H. Hu, High-performance stretchable yarn supercapacitor based on PPy@ CNTs@ urethane elastic fiber core spun yarn, *Nano Energy*, 2016, **27**, 230–237.
- 150 X. Wang, Q. Guo, X. Cai, S. Zhou, B. Kobe and J. Yang, Initiator-integrated 3D printing enables the formation of complex metallic architectures, *ACS Appl. Mater. Interfaces*, 2013, **6**(4), 2583–2587.
- 151 M. Lee, B. H. Wee and J. D. Hong, High performance flexible supercapacitor electrodes composed of ultralarge graphene sheets and vanadium dioxide, *Adv. Energy Mater.*, 2014, 1401372.
- 152 G. Xu, Y. Tian, X. Wei, L. Yang and P. K. Chu, Free-standing electrodes composed of carbon-coated Li<sub>4</sub>Ti<sub>5</sub>O<sub>12</sub> nanosheets and reduced graphene oxide for advanced sodium ion batteries, *J. Power Sources*, 2017, **337**, 180–188.
- 153 G. Hasegawa, K. Kanamori, T. Kiyomura, H. Kurata, K. Nakanishi and T. Abe, Hierarchically Porous Li<sub>4</sub>Ti<sub>5</sub>O<sub>12</sub> Anode Materials for Li-and Na-Ion Batteries: Effects of Nanoarchitectural Design and Temperature Dependence of the Rate Capability, *Adv. Energy Mater.*, 2015, **5**, 1400730.
- 154 L. Yu, H. B. Wu and X. W. D. Lou, Mesoporous Li<sub>4</sub>Ti<sub>5</sub>O<sub>12</sub> hollow spheres with enhanced lithium storage capability, *Adv. Mater.*, 2013, **25**(16), 2296–2300.
- 155 Y.-Q. Wang, L. Gu, Y.-G. Guo, H. Li, X.-Q. He, S. Tsukimoto, Y. Ikuhara and L.-J. Wan, Rutile-TiO<sub>2</sub> nanocoating for a high-rate Li<sub>4</sub>Ti<sub>5</sub>O<sub>12</sub> anode of a lithium-ion battery, *J. Am. Chem. Soc.*, 2012, **134**(18), 7874–7879.
- 156 K.-T. Kim, C.-Y. Yu, C. S. Yoon, S.-J. Kim, Y.-K. Sun and S.-T. Myung, Carbon-coated Li<sub>4</sub>Ti<sub>5</sub>O<sub>12</sub> nanowires showing high rate capability as an anode material for rechargeable sodium batteries, *Nano Energy*, 2015, **12**, 725–734.
- 157 Y. Ma, B. Ding, G. Ji and J. Y. Lee, Carbon-encapsulated F-doped Li<sub>4</sub>Ti<sub>5</sub>O<sub>12</sub> as a high rate anode material for Li+ batteries, *ACS Nano*, 2013, **7**(12), 10870–10878.
- 158 Y. Yang, B. Qiao, X. Yang, L. Fang, C. Pan, W. Song, H. Hou and X. Ji, Lithium titanate tailored by cathodically induced graphene for an ultrafast lithium ion battery, *Adv. Funct. Mater.*, 2014, **24**(27), 4349–4356.
- 159 H.-G. Jung, S.-T. Myung, C. S. Yoon, S.-B. Son, K. H. Oh, K. Amine, B. Scrosati and Y.-K. Sun, Microscale spherical carbon-coated Li<sub>4</sub>Ti<sub>5</sub>O<sub>12</sub> as ultra high power anode material for lithium batteries, *Energy Environ. Sci.*, 2011, **4**(4), 1345–1351.
- 160 C. Chen, H. Xu, T. Zhou, Z. Guo, L. Chen, M. Yan, L. Mai, P. Hu, S. Cheng and Y. Huang, Integrated Intercalation-Based and Interfacial Sodium Storage in Graphene-Wrapped Porous Li<sub>4</sub>Ti<sub>5</sub>O<sub>12</sub> Nanofibers Composite Aerogel, *Adv. Energy Mater.*, 2016, 1600322.
- 161 J. Liu, K. Song, P. A. van Aken, J. Maier and Y. Yu, Self-supported Li<sub>4</sub>Ti<sub>5</sub>O<sub>12</sub>-C nanotube arrays as high-rate and long-life anode materials for flexible Li-ion batteries, *Nano Lett.*, 2014, **14**(5), 2597–2603.
- 162 G. Xu, W. Li, L. Yang, X. Wei, J. Ding, J. Zhong and P. K. Chu, Highly-crystalline ultrathin Li<sub>4</sub>Ti<sub>5</sub>O<sub>12</sub> nanosheets decorated with silver nanocrystals as a high-performance anode material for lithium ion batteries, *J. Power Sources*, 2015, **276**, 247–254.
- 163 L. Wen, F. Li and H. M. Cheng, Carbon nanotubes and graphene for flexible electrochemical energy storage: from materials to devices, *Adv. Mater.*, 2016, **28**, 4306–4337.
- 164 R. Montazami, S. Liu, Y. Liu, D. Wang, Q. Zhang and J. R. Heflin, Thickness dependence of curvature, strain, and response time in ionic electroactive polymer actuators fabricated *via* layer-by-layer assembly, *J. Appl. Phys.*, 2011, **109**(10), 104301.
- 165 R. Montazami, V. Jain and J. R. Heflin, High contrast asymmetric solid state electrochromic devices based on layer-by-layer deposition of polyaniline and poly(aniline sulfonic acid), *Electrochim. Acta*, 2010, **56**(2), 990–994.
- 166 C. Meis, N. Hashemi and R. Montazami, Investigation of spray-coated silver-microparticle electrodes for ionic electroactive polymer actuators, *J. Appl. Phys.*, 2014, **115**(13), 134302.
- 167 M. Cakici, R. R. Kakarla and F. Alonso-Marroquin, Advanced electrochemical energy storage supercapacitors based on the flexible carbon fiber fabric-coated with uniform coral-like MnO<sub>2</sub> structured electrodes, *Chem. Eng. J.*, 2017, **309**, 151–158.
- 168 H. Gwon, H.-S. Kim, K. U. Lee, D.-H. Seo, Y. C. Park, Y.-S. Lee, B. T. Ahn and K. Kang, Flexible energy storage devices based on graphene paper, *Energy Environ. Sci.*, 2011, **4**(4), 1277–1283.
- 169 H. Mianehrow, S. Sabury, A. Bazargan, F. Sharif and S. Mazinani, A flexible electrode based on recycled paper pulp and reduced graphene oxide composite, *J. Mater. Sci.: Mater. Electron.*, 2017, 1–7.
- 170 H.-K. Seo, T.-S. Kim, C. Park, W. Xu, K. Baek, S.-H. Bae, J.-H. Ahn, K. Kim, H. C. Choi and T.-W. Lee, Value-added synthesis of graphene: recycling industrial carbon waste into electrodes for high-performance electronic devices, *Sci. Rep.*, 2015, **5**, 16710.
- 171 H. Koga, H. Tonomura, M. Nogi, K. Suganuma and Y. Nishina, Fast, scalable, and eco-friendly fabrication of an energy storage paper electrode, *Green Chem.*, 2016, **18**(4), 1117–1124.
- 172 H.-J. Chu, C.-Y. Lee and N.-H. Tai, Green reduction of graphene oxide by Hibiscus sabdariffa L. to fabricate flexible graphene electrode, *Carbon*, 2014, **80**, 725–733.
- 173 L. Qiu, D. Liu, Y. Wang, C. Cheng, K. Zhou, J. Ding, V.-T. Truong and D. Li, Mechanically Robust, Electrically Conductive and Stimuli-Responsive Binary Network Hydrogels Enabled by Superelastic Graphene Aerogels, *Adv. Mater.*, 2014, **26**(20), 3333–3337.
- 174 Z.-S. Wu, S. Yang, Y. Sun, K. Parvez, X. Feng and K. Müllen, 3D Nitrogen-Doped Graphene Aerogel-Supported Fe<sub>3</sub>O<sub>4</sub> Nanoparticles as Efficient Electrocatalysts for the Oxygen Reduction Reaction, *J. Am. Chem. Soc.*, 2012, **134**(22), 9082–9085.

- 175 Z. Chen, H. Li, R. Tian, H. Duan, Y. Guo, Y. Chen, J. Zhou, C. Zhang, R. Dugnani and H. Liu, Three dimensional Graphene aerogels as binder-less, freestanding, elastic and high-performance electrodes for lithium-ion batteries, *Sci. Rep.*, 2016, **6**, 27365.
- 176 J. Tang, J. Yang, X. Zhou, H. Yao and L. Zhou, A porous graphene/carbon nanowire hybrid with embedded SnO<sub>2</sub> nanocrystals for high performance lithium ion storage, *J. Mater. Chem. A*, 2015, **3**(47), 23844–23851.
- 177 D. Wei, Writable electrochemical energy source based on graphene oxide, *Sci. Rep.*, 2015, **5**, 15173.
- 178 R. Liang, H. Cao, D. Qian, J. Zhang and M. Qu, Designed synthesis of SnO<sub>2</sub>-polyaniline-reduced graphene oxide nanocomposites as an anode material for lithium-ion batteries, *J. Mater. Chem.*, 2011, **21**(44), 17654–17657.
- 179 S. Lv, F. Fu, S. Wang, J. Huang and L. Hu, Eco-friendly wood-based solid-state flexible supercapacitors from wood transverse section slice and reduced graphene oxide, *Electron. Mater. Lett.*, 2015, **11**(4), 633–642.
- 180 L. Lima, C. Matos, L. Gonçalves, R. Salvatierra, C. Cava, A. Zarbin and L. Roman, Water based, solution-processable, transparent and flexible graphene oxide composite as electrodes in organic solar cell application, *J. Phys. D: Appl. Phys.*, 2016, **49**(10), 105106.
- 181 H. Wang, D. Zhang, T. Yan, X. Wen, L. Shi and J. Zhang, Graphene prepared *via* a novel pyridine-thermal strategy for capacitive deionization, *J. Mater. Chem.*, 2012, **22**(45), 23745–23748.
- 182 J. Wang, W. Dou, X. Zhang, W. Han, X. Mu, Y. Zhang, X. Zhao, Y. Chen, Z. Yang, Q. Su, E. Xie, W. Lan and X. Wang, Embedded Ag quantum dots into interconnected Co<sub>3</sub>O<sub>4</sub> nanosheets grown on 3D graphene networks for high stable and flexible supercapacitors, *Electrochim. Acta*, 2017, **224**, 260–268.
- 183 S.-H. Lee, D. Kang and I.-K. Oh, Multilayered graphene-carbon nanotube-iron oxide three-dimensional heterostructure for flexible electromagnetic interference shielding film, *Carbon*, 2017, **111**, 248–257.
- 184 P. Liu, T. Yan, J. Zhang, L. Shi and D. Zhang, Separation and recovery of heavy metal ions and salt ions from wastewater by 3D graphene-based asymmetric electrodes *via* capacitive deionization, *J. Mater. Chem. A*, 2017, **5**(28), 14748–14757.
- 185 H. Wang, T. Yan, P. Liu, G. Chen, L. Shi, J. Zhang, Q. Zhong and D. Zhang, In situ creating interconnected pores across 3D graphene architectures and their application as high performance electrodes for flow-through deionization capacitors, *J. Mater. Chem. A*, 2016, **4**(13), 4908–4919.
- 186 R. Liu, L. Ma, S. Huang, J. Mei, J. Xu and G. Yuan, A flexible polyaniline/graphene/bacterial cellulose supercapacitor electrode, *New J. Chem.*, 2017, **41**, 857–864.
- 187 X. Ye, Q. Zhou, C. Jia, Z. Tang, Y. Zhu and Z. Wan, Producing large-area, foldable graphene paper from graphite oxide suspensions by *in situ* chemical reduction process, *Carbon*, 2017, **114**, 424–434.
- 188 B. Mehrabi-Matin, S. Shahrokhian and A. Iraji-zad, Silver Fiber Fabric as the Current Collector for Preparation of Graphene-Based Supercapacitors, *Electrochim. Acta*, 2017, **227**, 246–254.
- 189 Y.-X. Chen, P.-C. Chuang and R.-C. Wang, Cu particles induced distinct enhancements for reduced graphene oxide-based flexible supercapacitors, *J. Alloys Compd.*, 2017, **701**, 603–611.
- 190 P. Pattanauwat and D. Aht-ong, Controllable morphology of polypyrrole wrapped graphene hydrogel framework composites *via* cyclic voltammetry with aiding of poly (sodium 4-styrene sulfonate) for the flexible supercapacitor electrode, *Electrochim. Acta*, 2017, **224**, 149–160.
- 191 A. C. Ferrari, J. Meyer, V. Scardaci, C. Casiraghi, M. Lazzeri, F. Mauri, S. Piscanec, D. Jiang, K. Novoselov and S. Roth, Raman spectrum of graphene and graphene layers, *Phys. Rev. Lett.*, 2006, **97**(18), 187401.
- 192 S. Harada, W. Honda, T. Arie, S. Akita and K. Takei, Fully printed, highly sensitive multifunctional artificial electronic whisker arrays integrated with strain and temperature sensors, *ACS Nano*, 2014, **8**(4), 3921–3927.
- 193 K. Lee, J. Park, M.-S. Lee, J. Kim, B. G. Hyun, D. J. Kang, K. Na, C. Y. Lee, F. Bien and J.-U. Park, In-situ synthesis of carbon nanotube-graphite electronic devices and their integrations onto surfaces of live plants and insects, *Nano Lett.*, 2014, **14**(5), 2647–2654.
- 194 G. Yang, C. Lee, J. Kim, F. Ren and S. J. Pearton, Flexible graphene-based chemical sensors on paper substrates, *Phys. Chem. Chem. Phys.*, 2013, **15**(6), 1798–1801.
- 195 G. Zhu, W. Q. Yang, T. Zhang, Q. Jing, J. Chen, Y. S. Zhou, P. Bai and Z. L. Wang, Self-powered, ultrasensitive, flexible tactile sensors based on contact electrification, *Nano Lett.*, 2014, **14**(6), 3208–3213.
- 196 K. Elouarzaki, M. Bourourou, M. Holzinger, A. Le Goff, R. S. Marks and S. Cosnier, Freestanding HRP-GOx redox buckypaper as an oxygen-reducing biocathode for biofuel cell applications, *Energy Environ. Sci.*, 2015, **8**(7), 2069–2074.
- 197 Y. Zang, F. Zhang, C.-a. Di and D. Zhu, Advances of flexible pressure sensors toward artificial intelligence and health care applications, *Mater. Horiz.*, 2015, **2**(2), 140–156.
- 198 Z. Bai, J. M. Mendoza Reyes, R. Montazami and N. Hashemi, On-chip development of hydrogel microfibers from round to square/ribbon shape, *J. Mater. Chem. A*, 2014, **2**(14), 4878–4884.
- 199 H. Acar, S. Çınar, M. Thunga, M. R. Kessler, N. Hashemi and R. Montazami, Study of Physically Transient Insulating Materials as a Potential Platform for Transient Electronics and Bioelectronics, *Adv. Funct. Mater.*, 2014, **24**(26), 4135–4143.
- 200 F. Sharifi, B. B. Patel, A. K. Dzuilko, R. Montazami, D. S. Sakaguchi and N. Hashemi, Polycaprolactone Microfibrous Scaffolds to Navigate Neural Stem Cells, *Biomacromolecules*, 2016, **17**(10), 3287–3297.
- 201 N. Hashemi and G. Ghaffary, A Proposed Sustainable Rural Development Index (SRDI): Lessons from Hajjij village Iran., *Tourism. Manag.*, 2017, **59**, 130–138.
- 202 C. R. Carter and D. S. Rogers, A framework of sustainable supply chain management: moving toward new theory, *Int. J. Phys. Distrib. Logist. Manag.*, 2008, **38**(5), 360–387.